Asian Journal of Chemistry; Vol. 37, No. 4 (2025), 893-908

ASIAN JOURNAL OF CHEMISTRY

https://doi.org/10.14233/ajchem.2025.33467

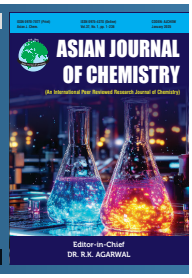

N-Alkylation Hybrids: Synthesis, Characterization, Anticancer Properties and Computational Insights

DEVENDAR BANOTHU[1], RAMU GUDA[2], RAMBABU PALABINDELA[3], PRABHAKAR MYADARAVENI[1], RAJASHEKAR KORRA[1] and MAMATHA KASULA[1,*]

[1]Department of Chemistry, Kakatiya University, Warangal-506009, India
[2]Advanced Centre of Research in High Energy Materials (ACRHEM), University of Hyderabad, Hyderabad-500046, India
[3]Department of Chemistry, Guru Nanak Institutions Technical Campus, Ibrahimpatanam-501506, India

*Corresponding author: E-mail: mamathakasula2016@gmail.com

Received: 3 February 2025; *Accepted*: 14 March 2025; *Published online*: 29 March 2025; AJC-21951

A series of (*E*)-2-(2-(anthracen-9-ylmethylene)hydrazinyl)-4-(pyrrolidin-1-ylmethyl)thiazole **(7a-l)** were synthesized and evaluated for their *in vitro* anticancer activity against three human cancer cell lines of MCF-7 (breast), A549 (lung) and HepG2 (liver). In this study, cisplatin served as the positive control. The results showed that the synthesized compounds **7c**, **7g**, **7i**, **7j** and **7l** demonstrated promising activity against all three cancer cell lines. Notably, compound **7j** exhibited higher activity than the standard drug cisplatin against MCF-7, A549 and HepG2, with IC_{50} values of 9.08 ± 0.32 µM, 5.92 ± 1.16 µM and 6.96 ± 0.13 µM, respectively. Molecular docking studies of the compounds **7g**, **7i** and **7j** with DNA topoisomerase II (PDB ID:3QX3) indicated strong affinity toward the target protein. Moreover, an *in silico* pharmacokinetic profile was generated for compounds **7g**, **7i** and **7j** using SWISS/ADMET and pkCSM. Furthermore, compounds **7g**, **7i** and **7j** were found to comply with the Lipinski, Ghose, Veber, Egan and Muegge rules. Based on the results, compound **7j** was characterized by and density functional theory (DFT) studies.

Keywords: Anthracene, Thiazole, Cyclic secondary amines, Anticancer, Docking studies, DFT studies, SWISS-ADMET studies.

INTRODUCTION

Uncontrolled cell division is a hallmark of cancer, a process characterized by abnormal cell growth and regeneration. Cancer begins in the human body when genetic and epigenetic abnormalities accumulate in healthy cells [1,2]. Despite the significant resources dedicated to cancer prevention and treatment, it remains one of the most pressing public health challenges worldwide. As a result, current medicinal chemistry is increasingly interested in the synthesis or development of stronger anticancer medications with fewer side effects [3,4]. Many effective anticancer drugs are available, including conventional chemotherapy agents that inhibit cell division and DNA replication. Regrettably, a large part of drugs currently on the market is not specific, which raises issues like the regular side effects [5,6].

Consequently, there is an increasing need for the discovery of more effective novel drugs that come with the minimal side effects. Remarkably, topoisomerase II and DNA are considered important targets of effective anticancer drugs [7,8]. Topoisomerase II (top II), one of the most specific and crucial regulators of DNA replication [9], plays its biological role *via* modification of DNA topology and regulation of DNA supercoiling [10].

On the other hand, anthracene containing compounds, as chemotherapeutic agents, have been studied in clinical trials [11]. Linking anthracene core with phosphonates has offered a large number of molecules with potential properties in the fields of biological sciences and materials [12,13]. Compounds of multi-anthracenes have brought the investigators attention towards their unique photophysical and chemical behaviour as organic functional material [14-16].

Anthracene, the simplest tricyclic aromatic compound, consists of three fused benzene rings. According to several studies, anthracene is non-carcinogenic and also easily biodegradable in soil particularly susceptible to degradation in

the presence of light [17]. Anthracene-based analogues have been used as fluorescent probes to study biological molecule binding [18,19]. These are used in the treatment of acute lymphoblastic leukemia, non Hodgkin's lymphoma, metastatic breast cancer and metastatic prostate cancer [20]. Building on this background and the distinct behaviour of an anthracene moiety when linked to biological molecules, we developed simple yet highly effective receptors, including amide, urea and thiourea moieties within Schiff base derivatives.

A well-known synthetic intermediate, chloroacetamide, which is a hydrazone-derived thiosemicarbazones has received remarkable attention due to their diverse agriculture applications and biological activities [21-30]. Another heterocyclic compound, thiazole is also a fascinating building block in the medicinal chemistry for the design and synthesis of biologically active derivatives [31-38] are reported. Many thiazole analogs exhibited very potent antitumor or cytotoxic activity and many of them have been specially designed to target specific pathways [39]. Some of these thiazole-containing compounds have progressed to clinical trials and are being explored for cancer therapy. Dabrafenib (inhibitor of enzyme B-RAF) [40], is examples of selective drug with tyrosine kinase inhibitory activity [41,42], Tiazofurin (induces apoptosis in human leukemia cells) and KUD773 (Induces apoptosis in human prostate cancer cells) [43] (Fig. 1).

The formation of 2º and 3º amino functionalities is a crucial step in the construction of polyamines on solid-phase supports and in the solid-phase organic synthesis of small molecules [44,45]. Piperazine which has two primary nitrogen atoms at its core, improves the pharmacokinetic features of therapeutic candidates because of its excellent pK_a [46]. The nitrogen sites enhance the water solubility of the drug-like molecules, which is essential for their bioavailability. When synthesizing and designing novel medications [47], keeping the pharmacodynamic and pharmacokinetic characteristics of drug-like compounds in balance is crucial. Remarkably, this ring contains pharmaceuticals that have FDA approval, such as gefitinib, bosutinib, imatinib, abemaciclib, dasatinib and reciletinib which help treat various cancer types [48-51].

DNA topoisomerase II was selected for docking studies in this study since it plays a major role in cell proliferation and is the key target for cancer cell proliferation prevention [52]. Mainly, a series of anthracene, thiazole and 2º amines hybrid compounds have shown that they act as inhibitors of the human DNA topoisomerase complex [53-58].

EXPERIMENTAL

All solvents, reagents and chemicals were used as received, without any purification. The reagents for the synthesis were sourced from S.D. Fine Chemicals, India and Sigma-Aldrich, USA. For thin-layer chromatography (TLC), RANKEM silica gel G and E-Merck precoated TLC plates were employed. The melting points were determined in open capillaries and are uncorrected. ^{1}H NMR spectra were recorded using a Bruker 400 MHz instrument, while ^{13}C NMR spectra were obtained on a Bruker 100 MHz instrument with TMS as internal standard. Elemental analysis was conducted with a Vario EL III CHNS analyzer. Mass spectra were recorded using Bruker Microsoft-Q II electrospray ionization-mass spectrometry (ESI-MS).

General procedure for the synthesis of anthracene-thiazole-linked *N*-alkyl heterocyclic aliphatic 2º amine (7a-l)

Synthesis of (*E*)-2-(2-(anthracen-9-ylmethylene)hydrazinyl)-4-(chloromethyl)thiazole (5a-b): The synthesis of targeted anthracene-thiazole-linked *N*-alkyl heterocyclic aliphatic secondary amines (**7a-l**) was accomplished in three steps. First, anthracene-9-carbaldehyde (**1**, 0.01 M), was added to thiosemicarbazide (**2**, 0.01 M) in methanol and the reaction mixture was refluxed for 3 h. The progress of the reaction was monitored by TLC. After cooling the reaction mixture to room temperature, the solid was filtered, yielding a yellow product **3a** with an 84% yield. Next, anthracene-9-carbaldehyde (**1**, 0.01 M) was reacted with 4-phenylthiosemicarbazide (**2b**, 0.01 M) in methanol solution and refluxed for 4 h. Upon completion of the reaction, the mixture was filtered and the yellow solid **3b** was obtained with an 86% yield. Finally, the thiazole ring was formed *via* a cyclization reaction by mixing compounds **3a-b** (0.01 M) with 1,3-dichloropropan-2-one (**4**, 0.015 M) in toluene

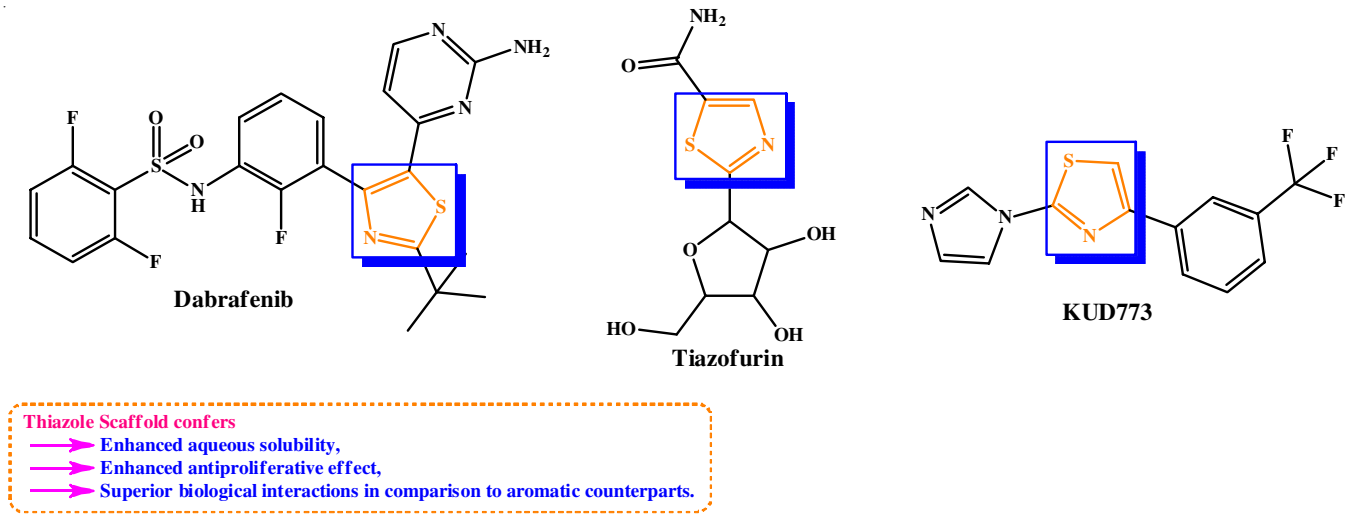

Fig. 1. Some clinically used thiazole-containing anticancer drugs

and the mixture was refluxed while stirring for 2.5 h. After the reaction was completed, the solvent was removed under reduced pressure and the residue was triturated with water. The resulting precipitate was filtered, washed with water and dried, yielding a yellow solid in 74-77% yield. The product was further purified by column chromatography using a dichloromethane/methanol mixture as eluent to give the final compounds **5a-b** (**Scheme-I**).

(*E*)-2-(2-(anthracen-9-ylmethylene)hydrazinyl)-4-(pyrrolidin-1-ylmethyl)thiazole (7a): *N*-Alkylation of compounds **6a-f** with various amines (0.02 M) was carried out by adding K_2CO_3 (0.125 M) to a stirred solution of compounds **5a-b** (0.01 M) in acetonitrile at room temperature. The reaction mixture was stirred for 2 to 4 h. Upon the completion of reaction (monitored by TLC), the mixture was cooled to room temperature and poured into a water/ethyl acetate (EtOAc) mixture. The organic layer was separated and washed with saturated $NaHCO_3$ solution and saturated brine solution. It was then dried over anhydrous sodium sulfate and filtered. The combined organic layers were transferred to a round-bottom flask and the solvent was evaporated under reduced pressure. The resulting residue was purified by column chromatography using silica gel (60-120 mesh) and a 2:3 ethyl acetate/hexane mixture as the eluent (**Scheme-I**). The final products **7a-l**, was obtained with yields ranging from 66% to 83%.

(*E*)-2-(2-(Anthracen-9-ylmethylene)hydrazinyl)-4-(pyrrolidin-1-ylmethyl)thiazole (7a): Yellow colour solid; yield: 68%; m.p.: 203-205 ºC; ^{1}H NMR (400 MHz, DMSO-d_6) δ ppm: 10.85 (s, 1H), 8.51 (s, 1H), 8.17 (8.06 (dd, *J* = 8.8, 5.6 Hz, 1H), 7.96 (s, 1H), 7.91 (s, 1H), 7.76 (s, 1H), 7.73 (d, *J* = 6.8 Hz, 2H), 7.37-7.30 (m, 2H), 6.73 (d, *J* = 2.2 Hz, 1H), 6.64 (s, 1H), 3.89 (s, 2H), 3.82 (s, 4H), 2.23 (s, 4H) ppm; ^{13}C NMR (100 MHz, DMSO-d_6) δ ppm: 168.26, 156.75, 151.25, 138.18, 137.89, 137.17, 133.89, 132.12, 129.82, 129.11, 126.82, 97.78; 54.72, 53.17, 23.03; MS (ESI): *m/z* 387.1654 $[M+H]^+$; CHN analysis for $C_{23}H_{22}N_4S$; calcd. (found) %: C, 71.47 (71.51); H, 5.74 (5.76); N, 14.50 (14.47).

(*E*)-2-(2-(Anthracen-9-ylmethylene)hydrazinyl)-4-(piperidin-1-ylmethyl)thiazole (7b): Yellow colour solid; 76% yield; m.p.: 217-219 ºC; ^{1}H NMR (400 MHz, DMSO-d_6) δ ppm: 10.99 (s, 1H), 8.54 (s, 1H), 8.16 (m, 1H), 8.02 (s, 1H), 7.94 (s, 1H), 7.67 (d, *J* = 6.3 Hz, 2H), 7.33-7.26 (m, 1H), 6.69 (d, *J* = 2.2 Hz, 1H), 6.58 (s, 1H), 3.86 (s, 2H), 2.86 (s, 4H), 2.72 (m, 6H); ^{13}C NMR (100 MHz, DMSO-d_6) δ ppm: 168.68, 156.68, 151.15, 134.96, 131.48, 130.46, 129.79, 129.34, 128.98, 127.62, 126.07, 104.19, 55.72, 52.23, 31.54, 28.32 ppm; MS (ESI): *m/z* 401.1712 $[M+H]^+$; CHN analysis for $C_{24}H_{24}N_4S$; calcd. (found) %: C, 71.97 (71.94); H, 6.04 (6.08); N, 13.99 (13.83).

(*E*)-4-((2-(2-(Anthracen-9-ylmethylene)hydrazinyl)-thiazol-4-yl)methyl)morpholine (7c): Yellow colour solid; yield: 66%; m.p.: 206-208 ºC; ^{1}H NMR (400 MHz, DMSO-d_6) δ ppm: 10.92 (s, 1H), 8.56 (s, 1H), 8.31 (s, 1H), 8.16 (d, *J*

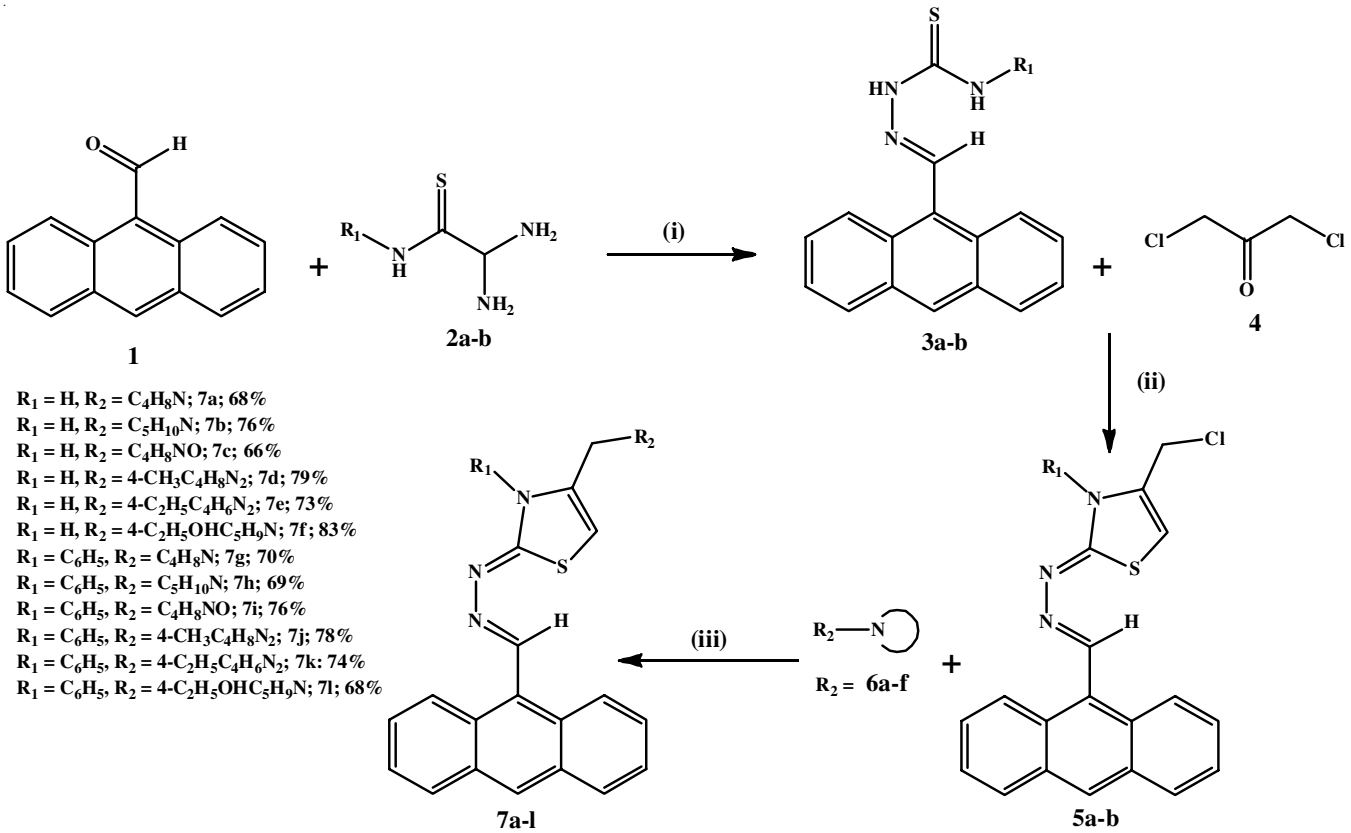

Reaction condition:

(i) anthracene-9-carbaldehyde (0.01M) (1), thiosemicarbazide (0.01 M) (2a-b), Methanol, reflux, 3-4 h

(ii) (*E*)-2-(anthracen-9-ylmethylene)hydrazine-1-carbothioamide (0.01 M) (3a-b), 1,3-dichloropropan-2-one (0.015 M) (4), reflux, 2.5 h

(iii) (*E*)-2-(2-(anthracen-9-ylmethylene)hydrazinyl)-4-(chloromethyl)thiazole (0.01 M) (5a-b), pyrrolidine (0.02 M) (6a-f), MeCN, K_2CO_3 (0.0125 M), r.t., 2-4 h

Scheme-I: Synthesis of anthracene-thiazole C-N linked secondary amines (**7a-l**)

= 7.7 Hz, 1H), 7.94 (s, 1H), 7.81 (d, *J* = 17.7 Hz, 1H), 7.71 (t, *J* = 10.0 Hz, 2H), 7.33 (m, 1H), 7.07 (t, *J* = 13.8 Hz, 2H), 7.00 (d, *J* = 8.0 Hz, 1H), 4.41 (s, 2H), 3.84 (s, 4H), 2.11 (s, 4H); ^{13}C NMR (100 MHz, DMSO-d_6) δ ppm: 169.70, 159.78, 151.50, 137.13, 134.82, 133.09, 131.14, 130.78, 124.58, 123.35, 120.48, 112.47, 66.42, 55.66, 51.07; MS (ESI): *m/z* = 403.1563 $[M+H]^+$; CHN analysis for $C_{23}H_{22}N_4OS$; calcd. (found) %: C, 68.63 (68.56); H, 5.51 (5.56); N, 13.92 (13.52).

(*E*)-2-(2-(Anthracen-9-ylmethylene)hydrazinyl)-4-((4-methylpiperazin-1-yl)methyl)thiazole (7d): Dark yellow colour solid; yield: 79%; m.p.: 214-216 ºC; ^{1}H NMR (400 MHz, DMSO-d_6) δ ppm: 11.10 (s, 1H), 8.58 (s, 1H), 8.23-8.12 (m, 2H), 7.92 (d, *J* = 9.7 Hz, 2H), 7.83 (s, 1H), 7.69 (d, *J* = 8.3 Hz, 2H), 7.43 (d, *J* = 3.0 Hz, 2H), 7.25-6.93 (m, 1H), 6.67 (s, 1H), 4.39 (s, 2H), 3.87 (s, 4H), 3.51 (s, 4H); ^{13}C NMR (100 MHz, DMSO-d_6) δ ppm: 169.95, 158.50, 154.35, 143.98, 130.28, 128.60, 127.98, 127.16, 126.31, 125.43, 117.01, 110.41, 56.59, 53.57, 50.47, 43.96; MS (ESI): *m/z* 416.1843 $[M+Na]^+$; CHN analysis for $C_{24}H_{25}N_5S$; calcd. (found) %: C, 69.37 (69.33); H, 6.06 (6.09); N, 16.85 (16.81).

(*E*)-2-(2-(Anthracen-9-ylmethylene)hydrazinyl)-4-((4-ethylpiperazin-1-yl)methyl)thiazole (7e): Orange colour solid; yield: 73%; m.p.: 221-223 ºC; ^{1}H NMR (400 MHz, DMSO-d_6) δ ppm: 10.91 (s, 1H), 8.53 (s, 1H), 8.32 (s, 1H), 8.14 (d, *J* = 2.3 Hz, 1H), 8.05 (d, *J* = 10.9 Hz, 1H), 7.73 (d, *J* = 6.3 Hz, 3H), 7.52-7.43 (m, 1H), 7.36-7.23 (m, 2H), 7.11 (m, 1H), 6.81 (s, 1H), 4.43 (s, 2H), 3.74 (s, 2H), 2.89 (s, 4H), 2.67 (s, 4H), 1.42 (t, *J* = 7.2 Hz, 3H); ^{13}C NMR (100 MHz, DMSO-d_6) δ ppm: 168.98, 153.28, 149.05, 133.22, 131.48, 129.81, 128.30, 127.16, 126.04, 125.62, 125.23, 110.13, 56.85, 51.03, 50.56, 45.96, 19.01; MS (ESI): *m/z* 430.1978 $[M+H]^+$; CHN analysis for $C_{25}H_{27}N_5S$; calcd. (found) %: C, 69.90 (69.96); H, 6.34 (69.96); N, 16.30 (18.64).

(*E*)-2-(1-((2-(2-(Anthracen-9-ylmethylene)hydrazinyl)-thiazol-4-yl)methyl)piperidin-4-yl)ethan-1-ol (7f): Pale yellow colour solid; yield: 83%; m.p.: 184-186 ºC; ^{1}H NMR (400 MHz, DMSO-d_6) δ ppm: 10.71 (s, 1H), 8.62 (s, 1H), 8.29 (s, 1H), 8.21 (d, *J* = 2.3 Hz, 1H), 8.03 (d, *J* = 11.3 Hz, 1H), 7.67 (d, *J* = 6.9 Hz, 3H), 7.53-7.44 (m, 1H), 7.38-7.25 (m, 2H), 7.11 (m, 1H), 6.73 (s, 1H), 4.72 (s, 1H), 4.48 (s, 2H), 3.93 (s, 2H), 3.86 (d, *J* = 1.6 Hz, 6H), 2.24-2.14 (m, 4H); ^{13}C NMR (100 MHz, DMSO-d_6) δ ppm: 168.94, 159.04, 153.50, 141.98, 131.33, 130.58, 129.59, 128.59, 127.98, 126.29, 116.99, 110.01. 59.06, 57.23, 56.62, 52.34, 52.09; MS (ESI): *m/z* 446.1984 $[M+H]^+$; CHN analysis for $C_{26}H_{28}N_4OS$; calcd. (found) %: C, 67.39 (67.36); H, 6.11 (6.14); N, 15.72 (15.76).

(Z)-2-(((*E*)-Anthracen-9-ylmethylene)hydrazono)-3-phenyl-4-(pyrrolidin-1-ylmethyl)-2,3-dihydrothiazole (7g): Dark yellow colour solid; yield: 72%; m.p.: 189-191 ºC; ^{1}H NMR (400 MHz, DMSO-d_6) δ ppm: 8.54 (s, 1H), 8.14 (dd, *J* = 7.7, 1.7 Hz, 1H), 7.98 (s, 1H), 7.92 (s, 1H), 7.79 (s, 1H), 7.70 (d, *J* = 6.8 Hz, 3H), 7.35-7.28 (m, 2H), 7.17-6.99 (m, 4H), 6.69 (d, *J* = 2.2 Hz, 1H), 6.58 (s, 1H), 3.94 (s, 2H), 3.84 (s, 4H), 2.10 (s, 4H); ^{13}C NMR (100 MHz, DMSO-d_6) δ ppm: 172.79, 160.48, 157.41, 142.06, 136.95, 136.73, 132.87, 132.26, 131.94, 131.33, 129.03, 128.42, 120.72, 110.71, 56.27, 55.66, 21.42; MS (ESI): *m/z* 463.1195 $[M+H]^+$; CHN analysis for $C_{29}H_{26}N_4S$; calcd. (found) %: C, 75.29 (75.33); H, 5.67 (5.71); N, 12.11 (12.15).

(Z)-2-(((*E*)-Anthracen-9-ylmethylene)hydrazono)-3-phenyl-4-(piperidin-1-ylmethyl)-2,3-dihydrothiazole (7h): Light orange solid; yield: 69%; m.p.: 196-198 ºC; ^{1}H NMR (400 MHz, DMSO-d_6) δ ppm: 8.54 (s, 1H), 8.16 (m, 1H), 8.02 (s, 1H), 7.94 (s, 1H), 7.67 (d, *J* = 6.3 Hz, 2H), 7.33-7.26 (m, 1H), 6.69 (d, *J* = 2.2 Hz, 1H), 7.19-6.93 (m, 5H), 6.58 (s, 1H), 3.86 (s, 2H), 2.86 (s, 4H), 2.72 (m, 6H); ^{13}C NMR (100 MHz, DMSO-d_6) δ ppm: 173.56, 157.63, 151.38, 137.26, 132.84, 130.21, 129.53, 129.37, 128.52, 128.18, 127.97, 127.20, 126.36, 108.81, 55.94, 52.68, 31.96, 28.98; MS (ESI): *m/z* 477.2035 $[M+H]^+$; CHN analysis for $C_{30}H_{28}N_4S$; calcd. (found) %: C, 75.60 (75.64); H, 5.92 (5.96); N, 11.75 (11.71).

4-(((Z)-2-(((*E*)-Anthracen-9-ylmethylene)hydrazono)-3-phenyl-2,3-dihydrothiazol-4-yl)methyl)morpholine (7i): Cream solid; yield: 76%; m.p.: 171-173 ºC; ^{1}H NMR (400 MHz, DMSO-d_6) δ ppm: 8.58 (s, 1H), 8.35 (d, *J* = 8.7 Hz, 2H), 8.18 (dd, *J* = 16.5, 12.4 Hz, 2H), 7.83 (s, 1H), 7.69 (d, *J* = 8.6 Hz, 2H), 7.42-7.28 (m, 3H), 7.17-7.05 (m, 4H), 6.78 (s, 1H), 3.95 (s, 2H), 3.85 (s, 4H), 3.53 (s, 4H); ^{13}C NMR (100 MHz, DMSO-d_6) δ ppm: 173.56, 157.04, 151.26, 144.20, 142.39, 137.00, 136.44, 133.08, 131.94, 131.59, 131.35, 131.04, 128.42, 120.22, 110.21, 66.47, 55.67, 51.15 ppm; MS (ESI): *m/z* 479.1821 $[M+Na]^+$; CHN analysis for $C_{29}H_{26}N_4OS$; calcd. (found) %: C, 72.78 (72.74); H, 5.48 (5.52); N, 11.71 (11.68).

(Z)-2-(((*E*)-Anthracen-9-ylmethylene)hydrazono)-4-((4-methylpiperazin-1-yl)methyl)-3-phenyl-2,3-dihydrothiazole (7j): Light Yellow solid; yield: 78%; m.p.: 167-169 ºC; ^{1}H NMR (400 MHz, DMSO-d_6) δ ppm: 8.55 (s, 1H), 8.20-8.13 (m, 2H), 7.94 (d, *J* = 9.7 Hz, 2H), 7.85 (s, 1H), 7.71 (d, *J* = 8.3 Hz, 2H), 7.34 (d, *J* = 3.0 Hz, 2H), 7.23-6.97 (m, 5H), 6.71 (s, 1H), 4.43 (s, 2H), 3.84 (s, 4H), 3.53 (s, 4H); ^{13}C NMR (100 MHz, DMSO-d_6) δ ppm: 173.58, 159.86, 157.07, 136.79, 136.22, 129.91, 129.35, 128.90, 128.57, 127.83, 126.70, 126.25, 122.02, 116.80, 108.85, 57.09, 53.76, 50.86, 44.05; MS (ESI): *m/z* 492.3011 $[M+Na]^+$; CHN analysis for $C_{30}H_{29}N_5S$; calcd. (found) %: C, 73.29 (73.33); H, 5.95 (5.91); N, 14.24 (14.27).

(Z)-2-(((*E*)-Anthracen-9-ylmethylene)hydrazono)-4-((4-ethylpiperazin-1-yl)methyl)-3-phenyl-2,3-dihydrothiazole (7k): Light orange solid; yield: 74%; m.p.: 181-183 ºC; ^{1}H NMR (400 MHz, DMSO-d_6) δ ppm: 8.58 (s, 1H), 8.16 (dd, *J* = 7.3, 1.7 Hz, 1H), 7.94 (s, 1H), 7.88 (s, 1H), 7.75 (s, 1H), 7.67 (d, *J* = 6.8 Hz, 3H), 7.33-7.4 (m, 2H), 7.13-6.95 (m, 4H), 6.67 (d, *J* = 2.4 Hz, 1H), 6.63 (s, 1H), 4.41 (s, 2H), 3.71 (s, 2H), 2.91 (s, 4H), 2.71 (s, 4H), 1.42 (t, *J* = 7.2 Hz, 3H); ^{13}C NMR (100 MHz, DMSO-d_6) δ ppm: 173.55, 161.62, 151.74, 137.22, 136.24, 134.58, 132.12, 130.28, 129.44, 128.54, 127.98, 127.16, 126.29, 108.90, 57.05, 51.45, 50.56, 46.15, 19.13; MS (ESI): *m/z* 506.2348 $[M+H]^+$; CHN analysis for $C_{31}H_{31}N_5S$; calcd. (found) %: C, 73.63 (73.61); H, 6.18 (6.23); N, 13.85 (13.81).

2-(1-(((Z)-2-(((*E*)-Anthracen-9-ylmethylene)hydrazono)-3-phenyl-2,3-dihydrothiazol-4-yl)methyl)piperidin-4-yl)ethan-1-ol (7l): Light yellow solid; yield: 68%; m.p.: 165-169 ºC; ^{1}H NMR (400 MHz, DMSO-d_6) δ ppm: 8.57 (s, 1H), 8.27 (s, 1H), 8.17 (d, *J* = 2.1 Hz, 1H), 8.01 (d, *J* = 11.2 Hz, 1H), 7.69 (d, *J* = 7.1 Hz, 3H), 7.50-7.41 (m, 1H), 7.40-7.27

(m, 2H), 7.08 (m, 5H), 6.78 (s, 1H), 4.78 (s, 1H), 4.46 (s, 2H), 3.95 (s, 2H), 3.84 (d, J = 1.4 Hz, 6H), 2.20-2.10 (m, 4H) ppm; ^{13}C NMR (100 MHz, DMSO-d_6) δ ppm: 173.69, 162.49, 159.91, 149.39, 144.11, 142.51, 137.11, 136.83, 133.93, 133.54, 132.91, 131.03, 129.11, 128.09, 120.46, 112.24, 61.11, 57.49, 55.65, 52.74, 51.25 ppm; MS (ESI): *m/z* 522.3129 $[M+Na]^+$; CHN analysis for $C_{32}H_{32}N_4OS$; ; calcd. (found) %: C, 71.37 (71.41); H, 5.99 (5.94); N, 13.42 (13.46).

MTT assay: The MTT (3-(4,5-dimethylthiazol-2-yl)-2,5-diphenyl-tetrazolium bromide) assay method was used to study in vitro anticancer activity of compounds (**7a-l**) against three human cancer cells MCF-7 (breast cancer), A549 (lung cancer), and HepG2 (liver cancer) with slight modifications [59]. Cells were acquired from the cell repository of the National Centre for Cell Sciences (NCCS), Pune, India. Briefly, all three cell lines were seeded at a density of 20,000 cells per well in a 96-well plate. Cells were grown in complete medium overnight and treated with varying concentrations (µmol/ml) compounds (**7a-l**) or DMSO as control. Each concentration was used in triplicate and each experiment was repeated three times. After various incubation times (24 h), the cells were incubated with MTT (2.5 mg/mL) in the CO_2 incubator for 2h until formazan crystal development. After removing the medium from each well, 100 µL of DMSO solvent was used to dissolve the formazan crystals (MTT metabolite) for 10 min at 37 ºC. Cisplatin was used as a standard. After thorough mixing, the plate was read at 570 nm for optical density with Multi-mode Varioskan instrument (Thermo-Scientific) based on which the percentage cell viability was calculated.

***In vitro* tyrosine kinase EGFR inhibitory activity:** Using erlotinib as a reference standard control, four potential candidates (**7c**, **7g**, **7i**, **7j** and **7l**) were investigated for EGFR kinase inhibitory activity. All the assay steps were followed as described in EGFR WT Kinase Assay Kit Catalogue no. 40321, respectively (BPS Biosciences, CA, USA) [60]. Briefly, 5x Kinase buffer 1, ATP and PTK substrate Poly (Glu: Tyr 4:1) (10 mg/mL) was thawed and master mixture (25 µL per well) was prepared with 6 µL 5x Kinase Buffer 1 + 1 µL ATP (500 µM) + 1 µL PTK substrate Poly (Glu: Tyr 4:1) (10 mg/mL) + 17 µL water. For initiation of the reaction, 25 µL of master mixture, 5 µL of inhibitor solution and 20 µL of EGFR enzyme were added per well. A positive control reaction was kept with buffer (without inhibitor) and the same amount of enzyme, while the blank reaction was kept with kinase buffer in the absence of enzyme. All the reaction samples were incubated at 30 ºC for 40 min and then 50 µL of Kinase-Glo Max reagent was added to each well, followed by 15 min incubation at room temperature in a dark condition. At the end of incubation, the luminescence was measured and the % inhibition values at each concentration were calculated considering the positive control response as 100%.

Molecular docking studies: AutoDock 4.2 was utilized for the molecular docking studies. The human DNA topoisomerase-II proteins (PDB ID: 3QX3) as the target and downloaded from the Protein Data Bank [61]. Ligands and water molecules were removed from the proteins and gasteiger charges were calculated after adding polar hydrogens. The ligands were drawn using ChemDraw 12, energy minimized and saved as .mol files. These files were then converted into .pdb files using Discovery Studio. A grid box with 60 points along each of the three coordinate axes was generated. The Lamarckian Genetic Algorithm (4.2) was employed to generate the .dpf file. The Cygwin interface was used to obtain the .dlg file, from which the results were extracted. Finally, the 2D and 3D images were rendered using Discovery Studio 4.1.0 software graphically visualization interface [62].

DFT studies: For the DFT methods, the Gaussian 09 software package was utilized. Quantum chemical calculations were performed using the DFT method with the three parameter hybrid functional (B3) for the exchange part and the Lee-Yang-Parr (LYP) correlation function with the B3LYP/6-311++G (d,p) basis set [63,64]. The structural parameters were obtained through geometry optimization. The Molecular Electrostatic Potential (MEP), which reflects the charge distribution of the molecule, was analyzed to identify its nucleophilic and electrophilic regions [65]. The visualization program was used to examine the shape of the HOMO-LUMO orbitals. Moreover, the energy distribution of the molecular orbitals, the HOMO-LUMO energy gap and Mulliken atomic charges were calculated for **7j** molecule.

RESULTS AND DISCUSSION

The synthesis of the targeted anthracene-thiazole-linked *N*-alkyl heterocyclic aliphatic secondary amines (**7a-l**) was carried out in three steps as depicted in **Scheme-I**. All the synthesized compounds were characterized by elemental analysis, infrared spectroscopy, ^{1}H & ^{13}C NMR, and ESI-MS.

SAR studies: The structure-activity relationship (SAR) was analyzed to assess the effect of substituents on the cyclic 2º amine attached to the thiazole core on anticancer activity. The compounds with electron-donating groups, compound **7j**, which features an N-phenyl ring on the thiazole and N-methyl group on 4-piperazine, demonstrated strong activity against all three cell lines, outperforming the standard drug.

Compound **7i** having N-phenyl ring of thiazole and morpholine substituent has displayed second highest activity in the series. But compounds **7g** and **7c** having N-phenyl ring of thiazole and pyrrolidine and without any substituent thiazole and morpholine substituent of compounds respectively have shown less activity compared to compounds **7j** and **7i**. Similarly, the compound **7h** N-phenyl ring of thiazole and piperidine group has shown least activity compared to all the above compounds. When without any substituent of thiazole and N-ethyl group of 4-piperazine, without any substituent thiazole and N-ethyl group of pyrrolidine (**7e** and **7a)** decreased the activity. But introducing N-phenyl ring of thiazole and piperidine ethanol of **7l** and introducing without any substituent thiazole and piperidine ethanol in case of **7f** had improved the activity to some extent but still they were less active than **7g** and **7c** having N-phenyl ring of thiazole and pyrrolidine, without any substituent thiazole and morpholine groups, respectively. The compounds **7b** and **7k** having without any substituent thiazole and piperidine groups and N-phenyl ring of thiazole and N-ethyl piperazine groups, respectively have shown less activity comp-

ared to without any substituent thiazole and N-methyl piperidine compound **7d**.

***In vitro* anticancer activity:** All the newly synthesized compounds **7a-l** were screened for *in vitro* anticancer activity against three cell lines *viz*. MCF-7 (breast cancer), A549 (lung cancer) and HepG2 (liver cancer) using the MTT assay, with results compared to the standard drug cisplatin. Compounds **7c**, **7g**, **7i**, **7j** and **7l** exhibited superior activity compared to cisplatin across the three cell lines, with IC_{50} values ranging from 3.02 μM to 6.8 μM. Specifically, compound **7j** displayed the highest anticancer activity against MCF-7, A549 and HepG2 cell lines, with IC_{50} values of 9.08 ± 0.32 μM, 5.92 ± 1.16 μM and 6.96 ± 0.13 μM, respectively. Compound **7i** showed the next highest activity against the same cell lines, with IC_{50} values of 15.21 ± 1.13 μM, 8.69 ± 0.55 μM and 13.53 ± 1.78 μM, respectively (Table-1).

TABLE-1
In vitro ANTICANCER ACTIVITY OF COMPOUNDS (**7a-l**) WITH IC_{50} (μM)

Compound	MCF-7	A549	HepG2
7a	58.74 ± 1.22	64.48 ± 0.18	64.86 ± 1.53
7b	65.54 ± 0.88	ND	ND
7c	37.34 ± 1.64	23.10 ± 0.19	43.05 ± 1.04
7d	63.11 ± 1.05	52.28 ± 0.89	51.02 ± 1.45
7e	55.44 ± 1.55	58.66 ± 1.08	ND
7f	52.33 ± 0.52	52.04 ± 1.24	67.14 ± 0.12
7g	20.79 ± 1.19	14.23 ± 0.61	22.87 ± 1.39
7h	ND	58.50 ± 0.77	ND
7i	15.21 ± 1.13	8.69 ± 0.55	13.53 ± 1.78
7j	9.08 ± 0.32	5.92 ± 1.16	6.96 ± 0.13
7k	68.70 ± 0.78	40.56 ± 1.56	ND
7l	40.46 ± 1.29	32.92 ± 1.04	50.68 ± 0.43
Cisplatin	6.25 ± 0.32	3.02 ± 0.19	5.01 ± 0.13

ND: Not determine. [a]IC_{50} after 26 h of incubation, each data represents as mean ± S.D values from three different experiments performed in triplicates. [b]MCF-7: human breast cancer cell line. [c]A549: lung cancer cell line. [d]HepG2: liver cancer cell line.

***In vitro* tyrosine kinase EGFR inhibitory activity:** We evaluated the inhibitory activity of the potent compounds (**7c**, **7g**, **7i**, **7j** and **7l**) against the tyrosine kinase EGFR to assess their potential. The results presented in Table-2 indicate that compound **7j** exhibit the highest EGFR tyrosine kinase inhibitory potency, with IC_{50} values of 0.32 ± 0.03 μM, respectively, outperforming the reference drug erlotinib, which has an IC_{50} value of 0.42 μM. On the other hand, compounds **7g** and **7i** showed slightly lower activity, with an IC_{50} value of 0.86 ± 0.05 μM and 0.56 ± 0.04 μM. Compounds **7c** and **7l** have shown moderate activity 2.85 ± 0.06 μM and 2.29 ± 0.07 μM, respectively compared to standard erlotinib. These findings provide strong evidence of the compounds' significant *in vitro* cytotoxicity activity.

TABLE-2
TYROSINE KINASE EGFR KINASE INHIBITORY ACTIVITY

Compound	IC_{50} (μM)* against EGFR
7c	2.85 ± 0.06
7g	0.86 ± 0.05
7i	0.56 ± 0.04
7j	0.32 ± 0.03
7l	2.29 ± 0.07
Erlotinib	0.42 ± 0.02

*Average of triplicates ± standard deviation

Molecular docking studies: Compounds **7g**, **7i** and **7j** with potential *in vitro* anticancer activity were examined for their interaction with human DNA topoisomerase–II (PDB ID: 3QX3) target in comparison to well-known inhibitor such as erlotinib [66-68]. The corresponding binding energies are also presented in Table-3. Compound **7g** shows a binding energy of -10.06 kcal/mol and formed two hydrogen bonds with LYS739 (3.08 Å) by nitrogen atom of diazene group and ASN742(3.38 Å) with sulfur atom of thiazole ring, pi-donar hydrogen bond with carbon atom of phenyl ring with GLN742 and phenyl ring with pi-Alkyl interaction with ALA869 and thiazole ring of pi-sulfur interactions with LYS739. The thiazole ring of pi-cation interacts with LYS739, anthracene ring interacts with LYS739 and MET782 residues as shown in Fig. 2. Compound **7i** has a displayed binding energy of -10.06 kcal/mol and exhibited one hydrogen bond with ARG743(3.39 Å) by the nitrogen atom of the diazene moiety and pi-cation GLU728 of phenyl ring and ARG743 of anthracene ring, pi-anion ARG743 of anthracene ring and pi-alkyl interactions are ARG729 of morpholine and PRO740 amino acid of morpholine, thiazole, phenyl and anthracene and pi-pi T-shaped interact with TRP856 and PHE1019 amino acid, as shown in Fig. 3. Compound **7j** (-10.67 kcal/mol) has formed one hydrogen bonding interactions observed by the nitrogen atom of the diazene moiety with TYR773 (2.98 Å) amino acids with carbon hydrogen bond interaction with GLU447 of piperazine ring, ASP557 and ASP559 interactions with methyl group of N-piperazine ring pi-sigma ARG729 of anthracene, pi-pi stacked ALA779 of phenyl ring, pi-sulfur HIS775 interaction with sulfur of thiazole ring, pi-alkyl interactions with ARG729, LYS739 and PRO740 of anthracene ring, HIS775 interaction with morpholine ring, ALA779 interaction with thiazole ring (Fig. 4).

The best docking pose and inhibitory potency of compounds **7g**, **7i** and **7j** and standard inhibitors against the human DNA topoisomerase–II protein were compared. The standard inhibitor etoposide displayed a binding energy of -7.68 kcal/mol and formed three hydrogen bonding interactions with

TABLE-3
MOLECULAR DOCKING RESULTS OF COMPOUNDS **7g**, **7i** AND **7j** WITH HUMAN DNA TOPOISOMERASE-II (PDB ID-3QX3)

Compound	Binding energy (kcal/mol)	Inhibition constant (nM)	Number of hydrogen bonds	Residues involved in hydrogen bonding (bond length, Å)
7g	-10.06	42.25 nM	2	LYS739 (3.08), ASN742 (3.38)
7i	-10.24	31.22 nM	1	ARG743 (3.39)
7j	-10.67	14.98 nM	1	TYR773 (2.98)
Etoposide	-7.68	2.35 μM	3	LYS739 (1.83), GLY741 (2.04), ILE872 (2.21)

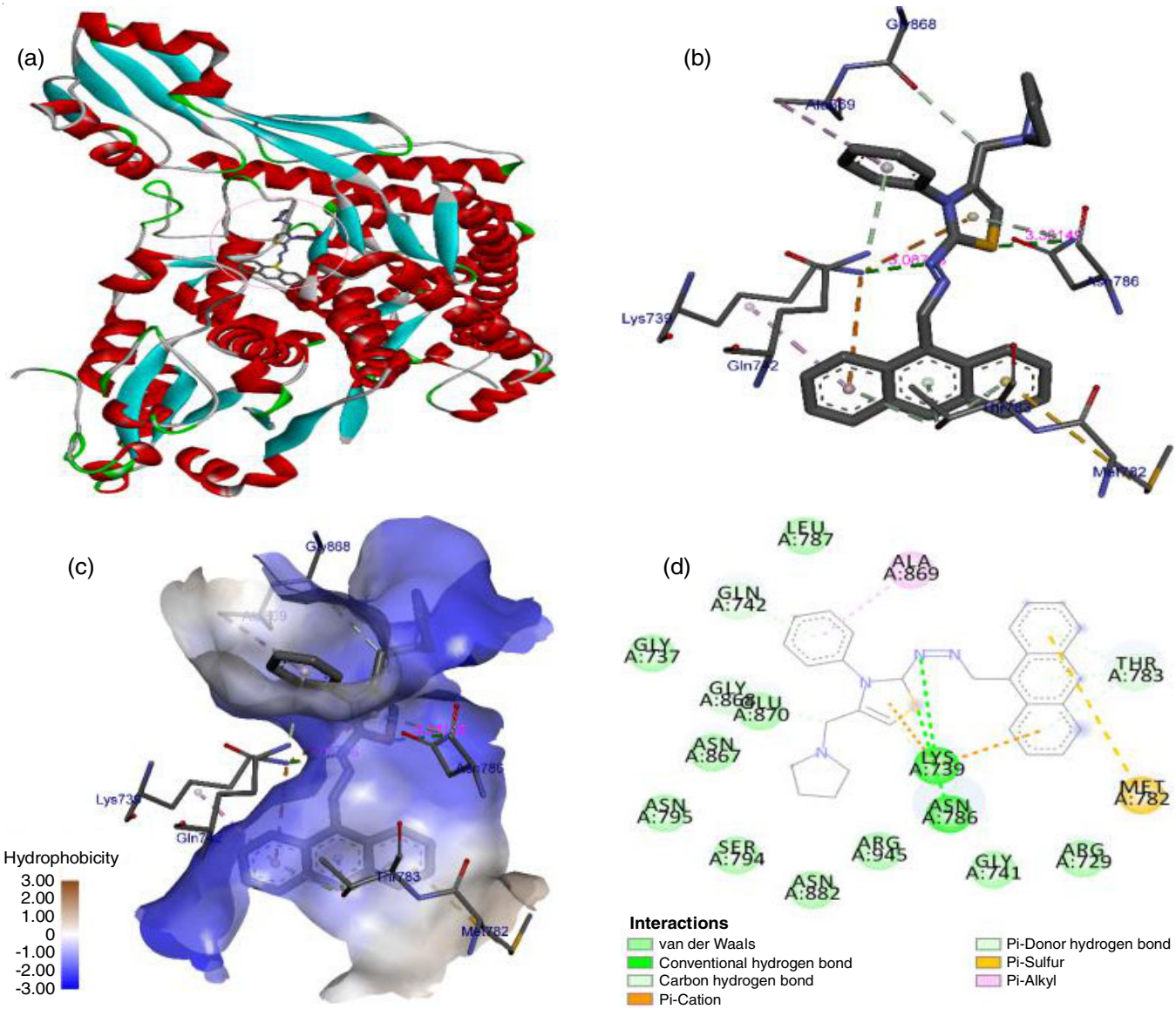

Fig. 2. Docking conformation of compound **7g** with EGFR, (a) protein with ligand interactions, (b) three-dimensional interactions, (c) hydrophobic interactions, (d) two-dimensional interactions

LYS739 (1.83 Å) by the oxygen atom of one methoxy group of phenyl ring and GLY741 (2.04 Å) by the oxygen atom of naphtho furanone group of etoposide, ILE872 (2.21 Å) by the hydroxy phenyl group of etoposide and remaining all are carbon hydrogen bond ASP726, GLY871 interactions with methoxy group of trimethoxy phenyl ring, alkyl and pi-alkyl ARG729 interaction with dioxolane ring, ALA779 interaction with phenyl ring of etoposide (Fig. 5).

Molecular geometry: The molecular structure and atom numbering of compound **7j** are shown in Fig. 6. This molecule contains 27 C–C bond lengths, 11 C–N bond lengths, 2 C–S bond lengths and 1 N–N bond length. The bond distances for the various benzene ring C–C bonds and C–H bonds of molecule **7j** are provided in Table-4. Among the 11 C–N bonds, C49–N56 and C50–N59 have the longest bond lengths of 1.4801 Å and 1.4755 Å, respectively. The C28–S31 and C30–S31 bonds have bond lengths of 1.8412 Å and 1.8186 Å, while the N26–N27 bond has the longest distance of 1.4134 Å. Additionally, the longest C–C bond length is C49–C52 at 1.5402 Å, whereas the shortest C–H bond length is C30–H44 at 1.072 Å. The largest bond angle observed was between atoms A (C30, C29, C33), measuring 143.7695º. Furthermore, the highest dihedral angle observed, D (50, 52, 56, 59), is 179.87º and indicates strong stabilizing conjugation between the C50 and C52 atoms, which are directly bonded to the more electronegative atoms.

Molecular electrical potential surface: The molecular electrostatic potential surface provides a 3D representation of charge distributions within the molecule. It displays the molecular size, shape and electrostatic potential highlighting negative, positive and neutral regions through colour gradients. Thus, a few physico-chemical properties (reactive properties of nucleic acids, including their component bases; biological recognition processes, including drug receptors and enzyme-substrate interactions; chemical carcinogenesis, referring specifically to polycyclic aromatic hydrocarbons and halogenated olefins and their epoxides, *etc*.) of a molecule can be analyzed using this method

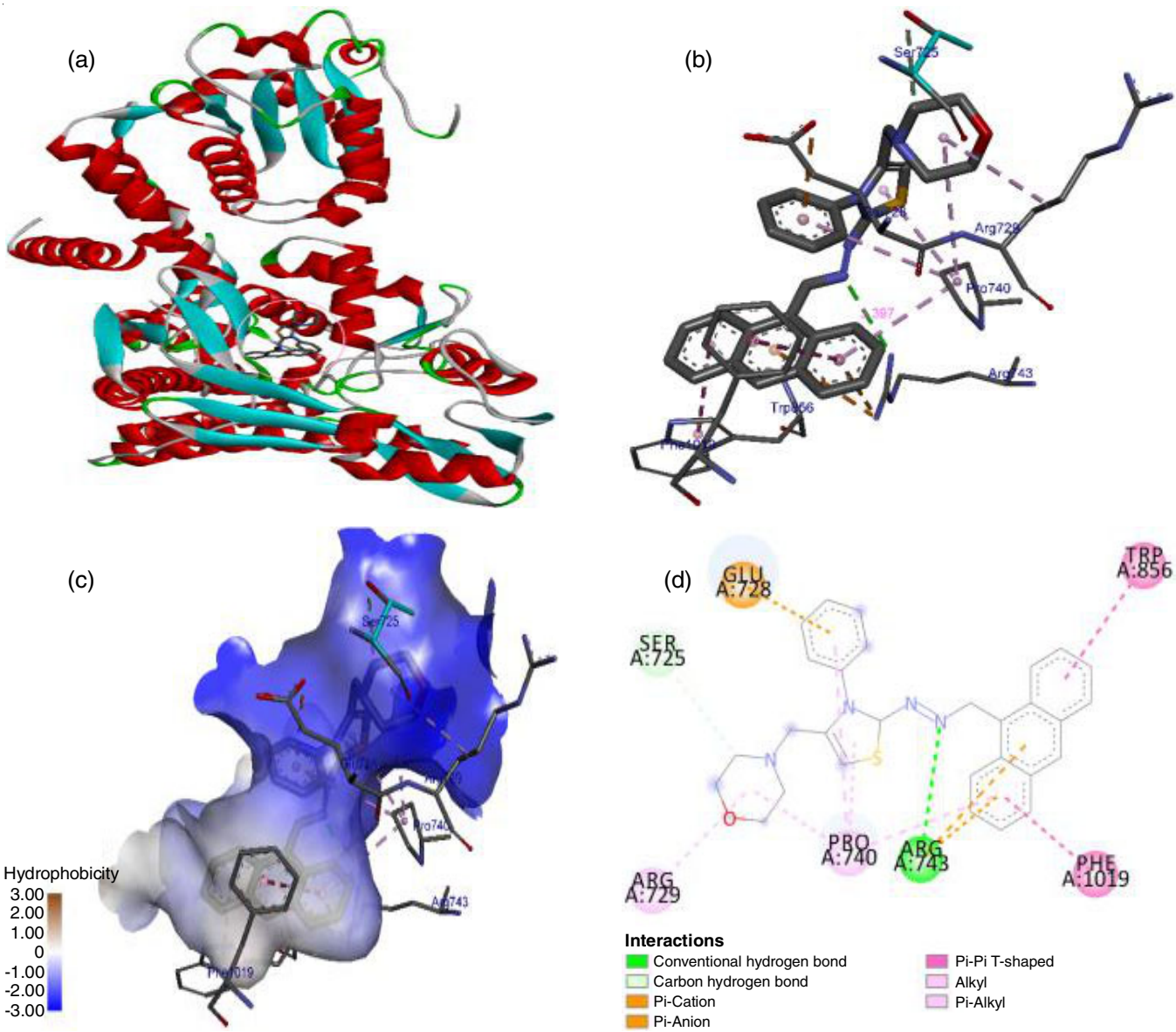

Fig. 3. Docking conformation of compound **7i** with EGFR, (a) protein with ligand interactions, (b) three-dimensional interactions, (c) hydrophobic interactions, (d) two-dimensional interactions

[69,70]. In Fig. 7, the different colours represent varying electrostatic potential values at the surface of compound **7j**. The electrostatic potential increases in the following order: red < orange < yellow < green < blue. The colour map ranges from -6.020 × 10^{-2} a.u. (deepest red) to 6.020 × 10^{-2} a.u. (deepest blue). The red colour indicates the strongest repulsion (electrophilic attack), while the blue colour signifies the strongest attraction (nucleophilic attack). Regions of negative electrostatic potential, typically associated with lone pairs on electronegative atoms, are observed around the nitrogen atoms and the diazene and thiazole nitrogen atoms. Conversely, positive electrostatic potential is seen over the hydrogen atoms bonded to carbon atoms. The highly allied light green colour represents the neutral region between the ends of red and blue [71].

Electronic properties: The molecular orbital analysis of E_{HOMO} and E_{LUMO} represents the HOMO and LUMO energies associated with chemical reactivity and stability [72,73]. The spatial distributions of the HOMO-LUMO orbitals for compound **7j** are displayed in Fig. 8. In general, global reactivity descriptors of molecules such as global hardness (η), ionization potential (I), chemical softness (S), electronegativity (χ) and global electrophilicity index (ω) were calculated using the HOMO and LUMO energy values of the molecule. These values are derived using the following formulas based on E_{HOMO} and E_{LUMO}, with the calculated results provided in Table-5. Global hardness and softness are the key properties that help assess molecular stability and reactivity. Molecules with a larger HOMO–LUMO energy gap are considered hard, while those with a smaller gap are classified as soft. Additionally, a low energy gap (ΔE) significantly influences the bioactivity and intermolecular charge transfer. The HOMO-LUMO energy gap is also linked to electronic excitation from the ground state to the excited state. Notably, compound **7j** exhibits a low energy gap of 3.31707 eV.

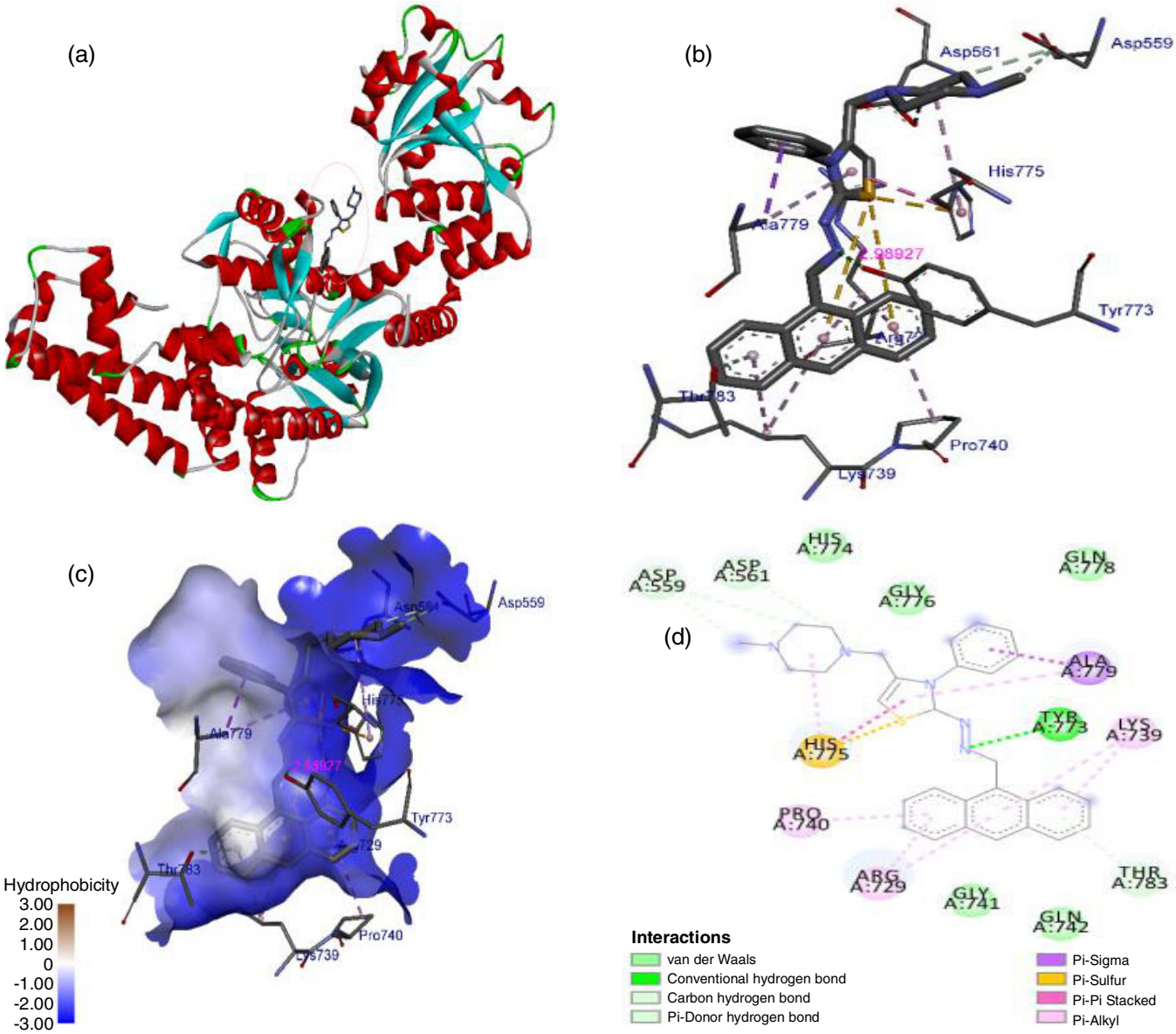

Fig. 4. Docking conformation of compound **7j** with EGFR, (a) protein with ligand interactions, (b) three-dimensional interactions, (c) hydrophobic interactions, (d) two-dimensional interactions

Mulliken atomic charges: These charges are important for the DFT calculations in optimized molecular geometry of molecular structure, dipole moment and electronic structure of molecule [74]. Mulliken atomic charges for compound **7j** were calculated using the DFT/B3LYP/6-311G++(d, p) basis set and the results are summarized in Table-6. The data reveals that seven carbon atoms C3, C8, C29, C30, C33, C45 and C62 carry positive charges, while 24 carbon atoms C1, C2, C4, C5, C6, C7, C9, C10, C11, C13, C14, C15, C24, C28, C34, C35, C36, C38, C40, C48, C49, C50, C52 and C54 bear negative charges. Similar to the Mulliken atomic charges, the sulfur atom S31 has a positive charge, while nitrogen atoms N26, N27, N32, O56 and N59 exhibit high electronegativity. Additionally, the positive charge distribution is observed on all the hydrogen atoms (Fig. 9).

***In silico* pharmacokinetic profile (ADMET):** The pharmacokinetic profiles of the three potent compounds **7g**, **7i** and **7j** were evaluated with the help of pkCSM and the drug likeness profiles of the same derivatives were also predicted with the aid of SWISS ADME/Tox [75,76]. The results are presented in Tables 7-9. The water solubility of the compounds was predicted using the log S parameter and all three compounds exhibited low water solubility (-2.893 to -6.755 log mol/L) due to their higher carbon content. The Caco2 permeability values ranged from 0.764 to 1.418 (log Papp in 10^{-6} cm/s). Moreover, the intestinal absorption percentages for compounds **7g**, **7i** and **7j** were 91.945%, 94.803% and 93.799%, respectively.

To evaluate the distribution of the derivatives, four key distribution variables were considered: distribution (log L/kg), percentage unbound, blood-brain barrier permeability (log BB) and CNS permeability. Compounds **7g**, **7i** and **7j** showed volume of distribution (log L/kg) values of 0.068, 1.191 and 1.200, respectively, while the unbound percentage values were 0.214, 0.221 and 0.191. Blood-brain barrier permeability was observed

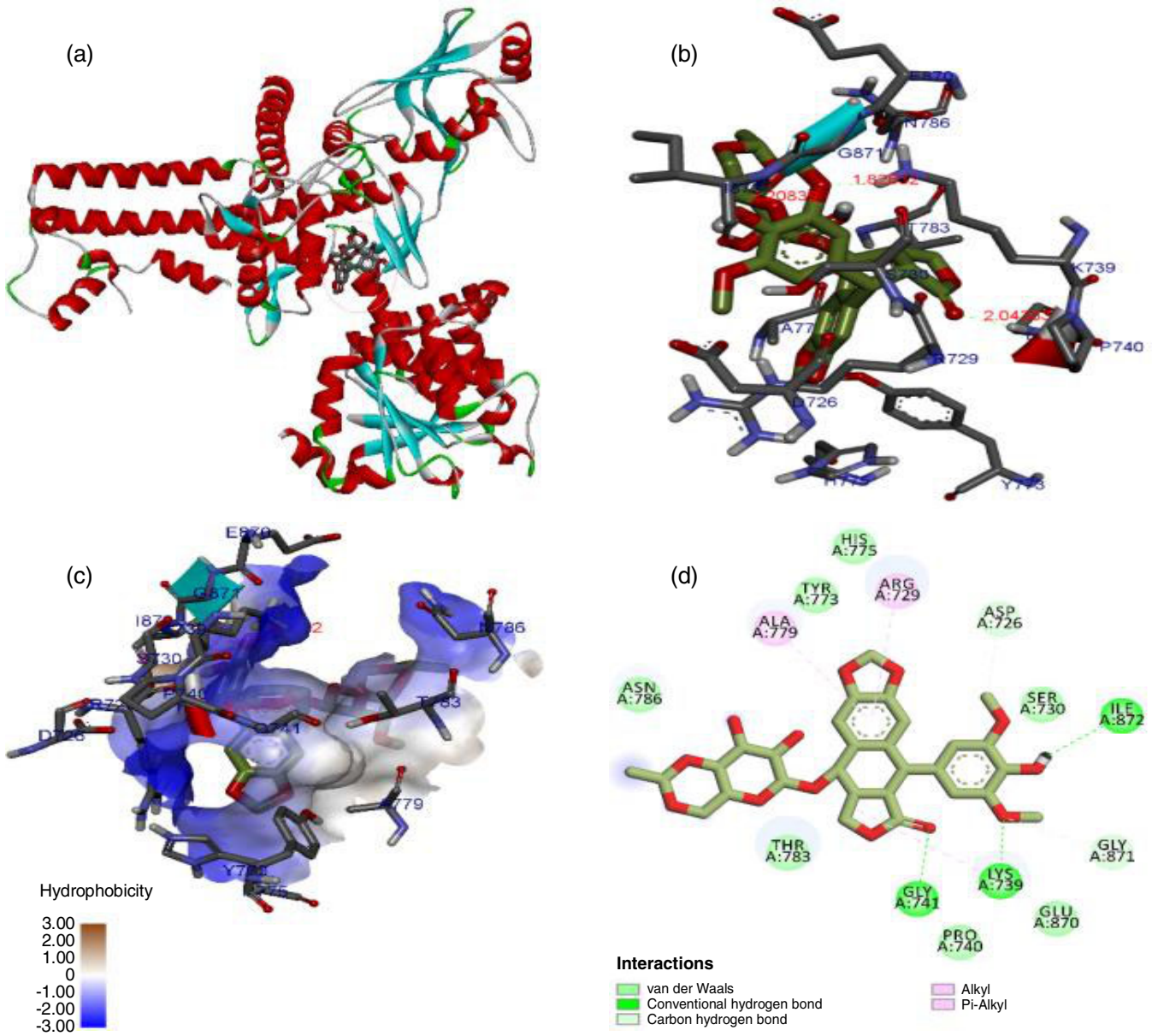

Fig. 5. Docking conformation of compound etoposide with 3, (a) protein with ligand interactions, (b) three-dimensional interactions, (c) hydrophobic interactions, (d) two-dimensional interactions

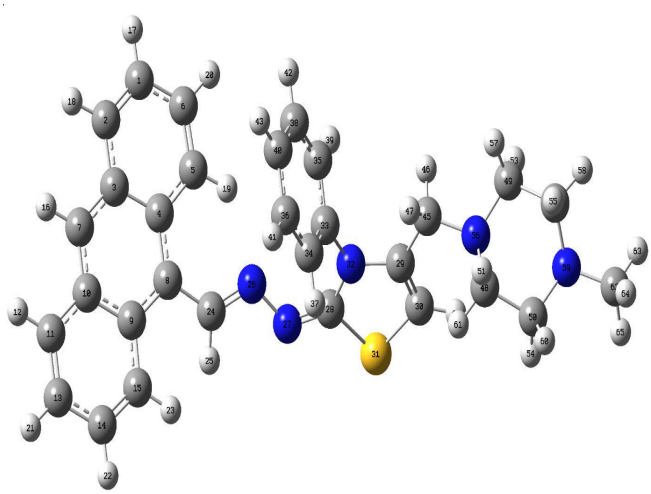

Fig. 6. Optimized geometrical structure of **7j** by using DFT calculations

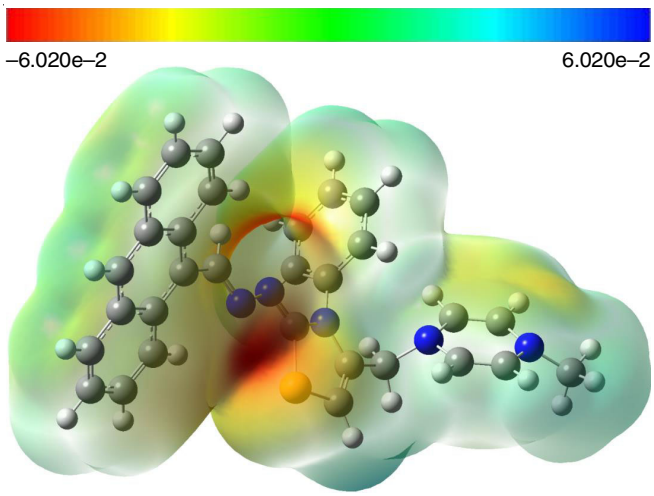

Fig. 7. Calculated MEP maps for **7j** molecule

TABLE-4
OPTIMIZED GEOMETRICAL PARAMETERS BOND LENGTH, BOND ANGLE OF **7j** MOLECULE B3LYP/6- 311G ++ (d, p)

Bond length	Theoretical value (Å)	Bond angle	Theoretical value (º)	Dihedral angle	Theoretical value (º)
C1–C2	1.3691	A (2,1,6)	119.6423	D (6,1,2,3)	-0.4566
C1–C6	1.4234	A (2,1,17)	120.5181	D (6,1,2,18)	179.3145
C1–H17	1.0821	A (6,1,17)	119.8381	D (17,1,2,3)	-179.9272
C2–C3	1.4324	A (1,2,3)	121.1388	D (17,1,2,18)	-0.1560
C2–H18	1.0831	A (1,2,18)	120.7188	D (2,1,6,5)	0.6058
C3–C4	1.4478	A (3,2,18)	118.1401	D (2,1,6,20)	-178.7987
C3–C7	1.3984	A (2,3,4)	119.508	D (17,1,6,5)	-179.9172
C4–C5	1.4331	A (2,3,7)	120.6688	D (17,1,6,20)	0.6782
C4–C8	1.4282	A (4,3,7)	119.8198	D (1,2,3,4)	-0.6624
C5–C6	1.3732	A (3,4,5)	117.2101	D (1,2,3,7)	179.1573
C5–H19	1.0763	A (3,4,8)	119.4381	D (18,2,3,4)	179.5606
C6–H20	1.0824	A (5,4,8)	123.3192	D (18,2,3,7)	-0.6197
C7–C10	1.398	A (4,5,6)	121.4372	D (2,3,4,5)	1.5755
C7–H16	1.084	A (4,5,19)	118.212	D (2,3,4,8)	-179.8379
C8–C9	1.43	A (6,5,19)	120.3361	D (7,3,4,5)	-178.2472
C8–C24	1.4655	A (1,6,5)	121.0539	D (7,3,4,8)	0.3394
C9–C10	1.4459	A (1,6,20)	119.3539	D (2,3,7,10)	-179.6769
C9–C15	1.435	A (5,6,20)	119.5917	D (2,3,7,16)	0.2721
C10–C11	1.4323	A (3,7,10)	121.7963	D (4,3,7,10)	0.1432
C11–H12	1.083	A (3,7,16)	119.1025	D (4,3,7,16)	-179.9078
C11–C13	1.3691	A (10,7,16)	119.1011	D (3,4,5,6)	-1.4594
C13–C14	1.4234	A (4,8,9)	119.6334	D (3,4,5,19)	177.2171
C13–H21	1.0818	A (4,8,24)	122.8617	D (8,4,5,6)	-179.9972
C14–C15	1.3728	A (9,8,24)	117.4321	D (8,4,5,19)	-1.3206
C14–H22	1.082	A (8,9,10)	119.8435	D (3,4,8,9)	-0.6981
C15–H23	1.0788	A (8,9,15)	123.1628	D (3,4,8,45)	176.5386
C24–H25	1.0868	A (10,9,15)	116.9724	D (5,4,8,9)	177.8006
C24–N26	1.3005	A (7,10,9)	119.4666	D (5,4,8,45)	4.9627
N26–N27	1.4134	A (7,10,11)	120.9551	D (4,5,6,1)	0.3861
N27–C28	1.2957	A (9,10,11)	119.5776	D (4,5,6,20)	179.7870
C28–S31	1.8412	A (10,11,12)	118.1224	D (19,5,6,1)	-178.3031
C28–N32	1.3996	A (10,11,13)	121.2282	D (19,5,6,20)	1.0978
C29–C30	1.3403	A (12,11,13)	120.649	D (3,7,10,9)	-0.2627
C29–N32	1.4272	A (11,13,14)	119.633	D (3,7,10,11)	-179.8355
C29–C45	1.5121	A (11,13,21)	120.5918	D (16,7,10,9)	179.7883
C30–S31	1.8186	A (14,13,21)	119.7734	D (16,7,10,11)	0.2155
C30–H44	1.072	A (13,14,15)	120.843	D (4,8,9,10)	0.5768
N32–C33	1.4492	A (13,14,22)	119.4542	D (4,8,9,15)	179.2103
C33–C34	1.397	A (15,14,22)	119.7009	D (45,8,9,10)	-176.5078
C33–C35	1.3955	A (9,15,14)	121.7231	D (45,8,9,15)	2.1257
C34–C36	1.3954	A (9,15,23)	119.6828	D (4,8,45,24)	142.8968
C34–H37	1.081	A (14,15,23)	118.5843	D (4,8,45,46)	-36.5396
C35–C38	1.396	A (8,24,25)	117.7009	D (9,8,45,24)	-39.9443
C35–H39	1.0811	A (8,24,26)	124.8729	D (9,8,45,46)	140.6193
C36–C40	1.3979	A (25,24,26)	117.4259	D (8,9,10,7)	-0.1002
C36–H41	1.0815	A (24,26,27)	112.7274	D (8,9,10,11)	179.4768
C38–C40	1.3973	A (26,27,28)	118.0688	D (15,9,10,7)	-178.8218
C38–H42	1.0814	A (27,28,31)	117.5335	D (15,9,10,11)	0.7551
C40–H43	1.0814	A (27,28,32)	133.5452	D (8,9,15,14)	-179.1572
C45–H46	1.0936	A (31,28,32)	108.9205	D (8,9,15,23)	2.1600
C45–H47	1.1019	A (30,29,32)	114.4172	D (10,9,15,14)	-0.4963
C45–N56	1.4636	A (30,29,33)	143.7695	D (10,9,15,23)	-179.1791
C48–C50	1.5393	A (30,29,45)	125.279	D (7,10,11,12)	-0.7443
C48–H51	1.1039	A (32,29,45)	120.3016	D (7,10,11,13)	179.1003
C48–N56	1.4691	A (33,29,45)	90.8604	D (9,10,11,12)	179.6818
C48–H61	1.0892	A (29,30,31)	112.3474	D (9,10,11,13)	-0.4736
C49–C52	1.5402	A (29,30,44)	126.3962	D (10,11,13,14)	-0.1032
C49–H53	1.0919	A (31,30,44)	121.2564	D (10,11,13,21)	-179.9903
C49–N56	1.4801	A (28,31,30)	89.3299	D (12,11,13,14)	179.7371
C49–H57	1.1029	A (28,32,29)	114.9782	D (12,11,13,21)	-0.1500
C50–H54	1.0927	A (28,32,33)	123.4557	D (11,13,14,15)	0.3808
C50–N59	1.4755	A (29,33,34)	118.9608	D (11,13,14,22)	-179.7896

C50–H60	1.1047	A (29,33,35)	111.361	D (21,13,14,15)	-179.7308
C52–H55	1.1056	A (32,33,34)	119.559	D (21,13,14,22)	0.0988
C52–H58	1.0905	A (32,33,35)	119.9176	D (13,14,15,9)	-0.0673
C52–N59	1.4634	A (34,33,35)	120.4745	D (13,14,15,23)	178.6028
N59–C62	1.4593	A (33,34,36)	119.6636	D (22,14,15,9)	-179.8961
C62–H63	1.0905	A (33,34,37)	119.4862	D (22,14,15,23)	-1.2260
C62–H64	1.1059	A (36,34,37)	120.8431	D (45,24,25,26)	179.1142
C62–H65	1.0913	A (33,35,38)	119.667	D (25,24,45,8)	-179.8600
		A (33,35,39)	119.4745	D (25,24,45,46)	-0.4273
		A (38,35,39)	120.8442	D (24,25,26,47)	179.6625
		A (34,36,40)	120.1384	D (24,25,26,48)	0.5085
		A (34,36,41)	119.7396	D (25,26,47,27)	-179.8060
		A (40,36,41)	120.1218	D (25,26,47,49)	-3.9127
		A (35,38,40)	120.1547	D (48,26,47,27)	-0.5240
		A (35,38,42)	119.7419	D (48,26,47,49)	175.3693
		A (40,38,42)	120.0961	D (25,26,48,60)	179.3026
		A (36,40,38)	119.8975	D (47,26,48,60)	0.0537
		A (36,40,43)	120.0571	D (47,27,28,29)	-164.3811
		A (38,40,43)	120.0437	D (47,27,28,30)	-47.7018
		A (29,45,46)	109.0776	D (47,27,28,39)	72.1203
		A (29,45,47)	109.8283	D (60,27,28,29)	16.5986
		A (29,45,56)	111.7158	D (60,27,28,30)	133.2778
		A (46,45,47)	105.892	D (60,27,28,39)	-106.9000
		A (46,45,56)	107.921	D (28,27,47,26)	-178.2151
		A (47,45,56)	112.179	D (28,27,47,49)	6.0694
		A (50,48,51)	110.4129	D (60,27,47,26)	0.9093
		A (50,48,56)	110.1325	D (60,27,47,49)	-174.8062
		A (50,48,61)	109.166	D (28,27,60,48)	178.2370
		A (51,48,56)	111.4874	D (28,27,60,61)	-0.6215
		A (51,48,61)	106.8938	D (47,27,60,48)	-0.8366
		A (56,48,61)	108.654	D (47,27,60,61)	-179.6951
		A (52,49,53)	109.8542	D (27,28,39,31)	-150.2657
		A (52,49,56)	110.943	D (27,28,39,32)	68.9484
		A (52,49,57)	108.2929	D (29,28,39,31)	87.997
		A (53,49,56)	108.2905	D (29,28,39,32)	-52.7889
		A (53,49,57)	107.799	D (30,28,39,31)	-29.4794
		A (56,49,57)	111.6062	D (30,28,39,32)	-170.2653
		A (48,50,54)	110.1036	D (34,31,33,37)	-0.8048
		A (48,50,59)	111.1773	D (34,31,33,40)	174.2961
		A (48,50,60)	108.3108	D (39,31,33,37)	-176.2734
		A (54,50,59)	108.4424	D (39,31,33,40)	-1.1725
		A (54,50,60)	107.337	D (33,31,39,28)	-134.6303
		A (59,50,60)	111.3982	D (33,31,39,32)	7.1918
		A (49,52,55)	110.2479	D (34,31,39,28)	49.6563
		A (49,52,58)	108.9356	D (34,31,39,32)	-168.5215
		A (49,52,59)	110.0024	D (36,32,35,38)	0.7719
		A (55,52,58)	106.5902	D (36,32,35,40)	-174.4724
		A (55,52,59)	112.2284	D (39,32,35,38)	176.8093
		A (58,52,59)	108.7199	D (39,32,35,40)	1.5650
		A (45,56,48)	115.4845	D (35,32,39,28)	134.2700
		A (48,56,49)	114.3712	D (35,32,39,31)	-7.3808
		A (50,59,52)	113.2059	D (36,32,39,28)	-49.4945
		A (50,59,62)	113.7926	D (36,32,39,31)	168.8547
		A (52,59,62)	115.9288	D (31,33,40,35)	-4.9092
		A (59,62,63)	109.9159	D (31,33,40,41)	146.4040
		A (59,62,64)	113.4103	D (37,33,40,35)	170.4400
		A (59,62,65)	109.474	D (37,33,40,41)	-38.2468
		A (63,62,64)	108.3118	D (32,35,40,33)	4.7118
		A (63,62,65)	107.8073	D (32,35,40,41)	-146.5918
		A (64,62,65)	107.7504	D (38,35,40,33)	-170.7718
				D (38,35,40,41)	37.9246
				D (33,40,41,42)	45.9306
				D (33,40,41,43)	164.0816
				D (33,40,41,44)	-74.9901
				D (35,40,41,42)	-163.8414

	D (35,40,41,43)	-45.6904
	D (35,40,41,44)	75.2379
	D (26,47,49,50)	93.9916
	D (26,47,49,51)	-85.2555
	D (27,47,49,50)	-90.5151
	D (27,47,49,51)	90.2377
	D (26,48,60,27)	0.4476
	D (26,48,60,61)	179.4002
	D (47,49,50,52)	-179.7522
	D (47,49,50,53)	0.7745
	D (51,49,50,52)	-0.51200
	D (51,49,50,53)	-179.9852
	D (47,49,51,54)	179.8325
	D (47,49,51,55)	0.6794
	D (50,49,51,54)	0.5861
	D (50,49,51,55)	-178.5670
	D (49,50,52,56)	0.1570
	D (49,50,52,57)	-179.8843
	D (53,50,52,56)	179.6225
	D (53,50,52,57)	-0.4189
	D (49,51,54,56)	-0.3034
	D (49,51,54,58)	-179.8422
	D (55,51,54,56)	178.8398
	D (55,51,54,58)	-0.6990
	D (50,52,56,54)	0.1225
	D (50,52,56,59)	179.8700
	D (57,52,56,54)	-179.8360
	D (57,52,56,59)	-0.0884
	D (51,54,56,52)	-0.0491
	D (51,54,56,59)	-179.7967
	D (58,54,56,52)	179.4878
	D (58,54,56,59)	-0.2598

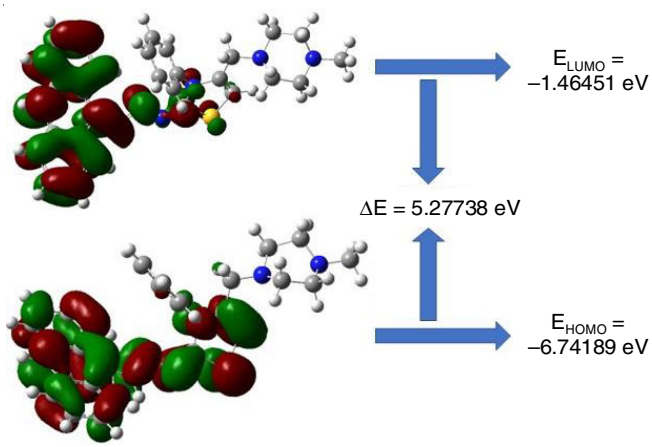

Fig. 8. Frontier molecular orbital energy gap of **7j**

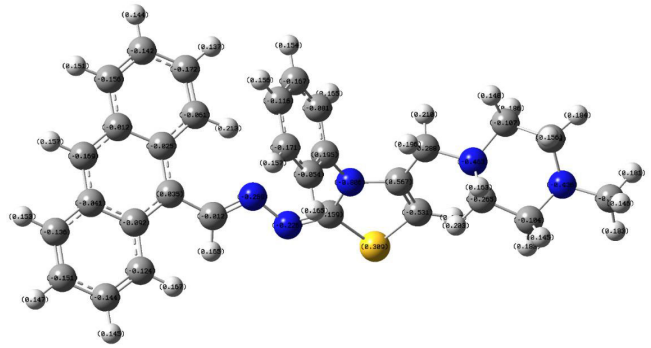

Fig. 9. Mulliken atomic charges of **7j** molecule

TABLE-5
GLOBAL REACTIVITY DESCRIPTORS OF **7j**

Property	B3LYP/6-311G++ (d, p)
E_{HOMO} (eV)	-6.74189
E_{LUMO} (eV)	-1.46451
Energy gap (eV)	5.27738
Ionization potential (I) (eV)	6.74189
Electron affinity (A) (eV)	1.46451
Electronegativity (χ) (eV)	4.10320
Global hardness (η) (eV)	2.63869
Chemical potential (μ) (eV)	-4.10320
Global electrophilicity (ω) (eV)	3.19026
Chemical softness (S) (eV)	0.37896

eV: Electron volt. ($I = -E_{HOMO}$), electron affinity ($A = -E_{LUMO}$), electronegativity ($\chi = (I + A)/2$), global hardness ($\eta = (I–A)/2$), chemical softness ($S = 1/\eta$), electronic chemical potential ($\mu = -(I+A)/2$) and electrophilicity ($\omega = \mu^2/2\eta$). All these parameters are listed in Table-5.

for all three derivatives, with log BB values of 0.622, -1.104 and -0.868 for **7g**, **7i** and **7j**, respectively. The CNS permeability (Log PS) values were between 0.684, -2.727 and -2.546.

In metabolic phase, compound **7g** interacts with CYP2D6 and CYP3A4 as both substrates and inhibitors and also inhibits CYP1A2. Compound **7i** interacts with CYP3A4 as both a substrate and inhibitor and CYP2D6 as a substrate. Compound **7j** shows similar behaviour, with CYP3A4 as a substrate and inhibitor, CYP2D6 as a substrate and CYP1A2 as an inhibitor. The excretion values for **7g**, **7i** and **7j** were 0.49, 0.633 and 0.641, respectively.

TABLE-6
CALCULATED MULLIKEN ATOMIC CHARGES OF **7j** MOLECULE

S. No.	Atoms	Mulliken atomic charges	S. No.	Atoms	Mulliken atomic charges	S. No.	Atoms	Mulliken atomic charges
1	C	-0.142	23	H	0.167	45	C	0.288
2	C	-0.156	24	C	-0.012	46	H	0.210
3	C	0.012	25	H	0.165	47	H	0.196
4	C	-0.025	26	N	-0.269	48	C	-0.265
5	C	-0.061	27	N	-0.226	49	C	-0.107
6	C	-0.172	28	C	-0.159	50	C	-0.104
7	C	-0.169	29	C	0.567	51	H	0.163
8	C	0.035	30	C	0.531	52	C	-0.258
9	C	-0.092	31	S	0.309	53	H	0.186
10	C	-0.041	32	N	-0.806	54	C	-0.104
11	C	-0.136	33	C	0.195	55	H	0.156
12	H	0.153	34	C	-0.081	56	N	-0.463
13	C	-0.151	35	C	-0.054	57	H	0.148
14	C	-0.144	36	C	-0.167	58	H	0.184
15	C	-0.124	37	H	0.165	59	N	-0.436
16	H	0.157	38	C	-0.171	60	H	0.146
17	H	0.144	39	H	0.165	61	H	0.203
18	H	0.151	40	C	-0.167	62	C	0.368
19	H	0.213	41	H	0.154	63	H	0.181
20	H	0.137	42	H	0.157	64	H	0.146
21	H	0.147	43	H	0.156	65	H	0.183
22	H	0.145	44	H	0.137			

TABLE-7
CALCULATION OF ADME PROPERTIES OF THE COMPOUNDS **7g**, **7i** AND **7j** USING pkCSM

Compd.	Absorption			Distribution				Metabolism (S = substrate; I = inhibitor)	Excretion Log (mL/min/kg)
	Log S (log mol/L)	Caco2 perm. (logPapp in 10^{-6} cm/s)	Int. abs. (% abs.)	V Dss (LogL/kg)	Fract. unb. (Fu)	BBB perm. (log BB)	CNS perm. (log PS)		
7g	-6.755	0.764	91.945	0.068	0.214	0.622	-0.684	CYP2D6 (S&I) CYP3A4 (S&I) CYP1A2(I)	0.49
7i	-2.974	1.418	94.803	1.191	0.221	-1.104	-2.727	CYP3A4 (S&I) CYP2D6 (S)	0.633
7j	-2.893	1.376	93.799	1.200	0.191	-0.868	-2.546	CYP2D6 (S) CYP3A4 (S&I) CYP1A2 (I)	0.641

Predicted physico-chemical properties of the compounds by the molinspiration.

TABLE-8
TOXICITY PREDICTION OF COMPOUNDS **7g**, **7i** AND **7j** USING pkCSM

Compd.	AMES toxicity	hERG I inhibitor	hERG II inhibitor	Hepato toxicity	Skin permeation	Max. tolerated dose (human); log (mg/kg/day)
7g	Yes	No	Yes	Yes	No	0.569
7i	No	No	Yes	Yes	No	0.517
7j	No	No	Yes	Yes	No	0.545

TABLE-9
DRUG LIKENESS PROFILE OF THE COMPOUNDS **7g**, **7i** AND **7j** CALCULATED USING SWISS/ADME

Compd.	Lipinski rule	Ghose rule	Veber rule	Egan rule	Muegge rule	Lead likeness	Bioavailability score
7g	Violation	Yes	–	–	–	–	–
7i	Yes	No;1violation: MR > 130	Yes	Yes	Yes	No; 1violation: MW > 350	0.55
7j	Yes	Yes	Yes	Yes	Yes	No; 1violation: MW > 350	0.55

Compounds **7g**, **7i** and **7j** are all hepatotoxic, however none of these compounds inhibit hERG I. Compound **7g** inhibits AMES, while compounds **7i** and **7j** do not. Moreover, all three compounds inhibit hERG II but do not affect skin permeability. The maximum tolerated dose (MTD) for compound **7g** is 0.569 (in log value of mg/kg/day), while compounds **7i** and **7j** have values of 0.517 and 0.545, respectively. Five filters (Lipinski rule, Ghose rule, Veber rule, Egan rule and Muegge rule) were applied to evaluate the drug-likeness of the compounds using SWISS/ADMET. Compounds **7g**, **7i** and **7j** satisfactorily completed four out of five criteria, however compound **7f** did not adhere to the Ghose rule. The overall bioavailability score for these compounds was 0.55.

Conclusion

The synthesis of hybrid compounds containing anthracene-thiazole linked cyclic 2º amines (**7a-l**) was successfully accomplished. The anticancer activity of synthesized compounds was evaluated on three human cancer cell lines *viz*. MCF-7 (breast), A-549 (lung) and HepG2 (liver). The anticancer assessment revealed that compounds **7g**, **7i** and **7j** showed more promising activity than cisplatin. Molecular docking studies indicated strong binding interactions between these compounds and the DNA topoisomerase-II protein receptor. Furthermore, compound **7j** was analyzed using density functional theory (DFT) with the B3LYP/6–311G++(d,p) basis set. Furthermore, compounds **7g**, **7i** and **7j** underwent *in silico* pharmacokinetic analysis using SWISS, ADMET and pkCSM, where all three compounds met the four criteria, except compound **7j**, which did not comply with the Ghose rule.

ACKNOWLEDGEMENTS

The authors thank National Institute of Technology (NITW), Warangal, India for recording ^{1}H NMR and ^{13}C NMR, Indian Institute of Technology, Jodhpur, Karwar, India, for mass spectral data, as well as the Department of Chemistry, Kakatiya University, Warangal, for providing research facilities. One of the authors, Devendar Banothu thanks the Council of Scientific & Industrial Research (CSIR) New Delhi, India, for financial support.

CONFLICT OF INTEREST

The authors declare that there is no conflict of interests regarding the publication of this article.

REFERENCES

1. K.P. Rakesh, H.K. Kumara, H.M. Manukumar and D.C. Gowda, *Bioorg. Chem.*, **87**, 252 (2019); https://doi.org/10.1016/j.bioorg.2019.03.038
2. B. Moku, L. Ravindar, K. Rakesh and H.L.J.B.C. Qin, *Bioorg. Chem.*, **86**, 513 (2019); https://doi.org/10.1016/j.bioorg.2019.02.030
3. S. Morgan, P. Grootendorst, J. Lexchin, C. Cunningham and D. Greyson, *Health Policy*, **100**, 4 (2011); https://doi.org/10.1016/j.healthpol.2010.12.002
4. Y. Chen, L. Liu, L. Xia, N. Wu, Y. Wang, H. Li, X. Chen, X. Zhang, Z. Liu, M. Zhu, Q. Liao and J. Wang, *J. Exp. Clin. Cancer Res.*, **41**, 44 (2022); https://doi.org/10.1186/s13046-022-02252-1
5. U.M. Ammar, M.S. Abdel-Maksoud and C.H. Oh, *Eur. J. Med. Chem.*, **158**, 144 (2018); https://doi.org/10.1016/j.ejmech.2018.09.005
6. F. Gao, X. Zhang, T. Wang and J. Xiao, *Eur. J. Med. Chem.*, **165**, 59 (2019); https://doi.org/10.1016/j.ejmech.2019.01.017
7. I.H. Eissa, A.M. El-Naggar and M.A. El-Hashash, *Bioorg. Chem.*, **67**, 43 (2016); https://doi.org/10.1016/j.bioorg.2016.05.006
8. Y. Pommier, E. Leo, H. Zhang and C. Marchand, *Chem. Biol.*, **17**, 421 (2010); https://doi.org/10.1016/j.chembiol.2010.04.012
9. J.L. Nitiss, *Nat. Rev. Cancer*, **9**, 327 (2009); https://doi.org/10.1038/nrc2608
10. L.F. Liu, *Annu. Rev. Biochem.*, **58**, 351 (1989); https://doi.org/10.1146/annurev.bi.58.070189.002031
11. M.S. Malik, R.I. Alsantali, R.S. Jassas, A.A. Alsimaree, R. Syed, M.A. Alsharif, K. Kalpana, M. Morad, I.I. Althagafi and S.A. Ahmed, *RSC Adv.*, **11**, 35806 (2021); https://doi.org/10.1039/d1ra05686g
12. M.Z.K. Baig, B. Prusti, S. Bhuin and M. Chakravarty, *hosphorus Sulfur Silicon Relat. Elem.*, **195**, 526 (2020); https://doi.org/10.1080/10426507.2020.1723098
13. I. Kraicheva, E. Vodenicharova, B. Shivachev, R. Nikolova, A. Kril, M. Topashka-Ancheva, I. Iliev, A. Georgieva, T. Gerasimova, T. Tosheva, E. Tashev, I. Tsacheva and K. Troev, *Phosphorus Sulfur Silicon Relat. Elem.*, **188**, 1535 (2013); https://doi.org/10.1080/10426507.2012.761986
14. A. Kastrati, F. Oswald, A. Scalabre and K.M. Fromm, *Photochem*, **3**, 227 (2023); https://doi.org/10.3390/photochem3020015
15. M. Yoshizawa and J.K. Klosterman, *Chem. Soc. Rev.*, **43**, 1885 (2014); https://doi.org/10.1039/C3CS60315F
16. J. Huang, J.H. Su and H. Tian, *J. Mater. Chem.*, **22**, 10977 (2012); https://doi.org/10.1039/c2jm16855c
17. Meenu, M. Rani and U. Shanker, *Environ. Sci.: Adv.*, **3**, 249 (2024); https://doi.org/10.1039/D3VA00245D
18. C.A. Terry, M.J. Fernández, L. Gude, A. Lorente and K.B. Grant, *Biochemistry*, **50**, 10375 (2011); https://doi.org/10.1021/bi200972c
19. P. Chinnaayya Swamy, J. Shanmugapriya, S. Singaravadivel, G. Sivaraman and D. Chellappa, *ACS Omega*, **3**, 12341 (2018); https://doi.org/10.1021/acsomega.8b01142
20. F.A. Holmes, L. Esparza, H.Y. Yap, A.U. Buzdar, R. George, Blumenschein and G.N. Hortobagyi, *Cancer Chemother. Pharmacol.*, **18**, 157 (1986); https://doi.org/10.1007/BF00262287
21. G. Vastag, S. Apostolov and B. Matijevic, *Iran. J. Pharm. Res.*, **17**, 100 (2018).
22. Ü.D. Özkay, Y. Özkay and Ö.D. Can, *Med. Chem. Res.*, **20**, 152 (2011); https://doi.org/10.1007/s00044-010-9300-y
23. T. Ertan, I. Yildiz, S. Ozkan, O. Temiz-Arpaci, F. Kaynak, I. Yalcin, E. Aki-Sener and U. Abbasoglu, *Bioorg. Med. Chem.*, **15**, 2032 (2007); https://doi.org/10.1016/j.bmc.2006.12.035
24. A. Bogdanovic, A. Lazic, S. Grujic, I. Dimkic, S. Stankovic and S. Petrovic, *Arh. Hig. Rada Toksikol.*, **72**, 70 (2021); https://doi.org/10.2478/aiht-2021-72-3483
25. H. Jawed, S.U.A. Shah, S. Jamall and S.U. Simjee, *Int. Immunopharmacol.*, **10**, 900 (2010); https://doi.org/10.1016/j.intimp.2010.04.028
26. M.A. Kaldrikyan, L.A. Grigoryan, R.G. Melik-Ogandzhanyan and F.G. Arsenyan, *Pharm. Chem. J.*, **43**, 242 (2009); https://doi.org/10.1007/s11094-009-0287-y
27. A. Hirashima, Y. Yoshii and M. Eto, *Agric. Biol. Chem.*, **55**, 2537 (1991); https://doi.org/10.1080/00021369.1991.10871030
28. H. Okamoto, S. Kato, T. Kobutani, M. Ogasawara, M. Konnai and T. Takematsu, *Agric. Biol. Chem.*, **55**, 2737 (1991); https://doi.org/10.1271/bbb1961.55.2737
29. F. Zaragoza and H. Stephensen, *J. Org. Chem.*, **64**, 2555 (1999); https://doi.org/10.1021/jo982070i
30. G. Sirasani and R.B. Andrade, *Org. Lett.*, **11**, 2085 (2009); https://doi.org/10.1021/ol9004799

31. A. Ayati, S. Emami, A. Asadipour, A. Shafiee and A. Foroumadi, *Eur. J. Med. Chem.*, **97**, 699 (2015); https://doi.org/10.1016/j.ejmech.2015.04.015
32. M. Djukic, M. Fesatidou, I. Xenikakis, A. Geronikaki, V.T. Angelova, V. Savic, M. Pasic, B. Krilovic, D. Djukic, B. Gobeljic, M. Pavlica, A. Djuric, I. Stanojevic, D. Vojvodic and L. Saso, *Chem. Biol. Interact.*, **286**, 119 (2018); https://doi.org/10.1016/j.cbi.2018.03.013
33. R.N. Sharma, F.P. Xavier, K.K. Vasu, S.C. Chaturvedi and S.S. Pancholi, *J. Enzyme Inhib. Med. Chem.*, **24**, 890 (2009); https://doi.org/10.1080/14756360802519558
34. S. Bondock, T. Naser and Y.A. Ammar, *Eur. J. Med. Chem.*, **62**, 270 (2013); https://doi.org/10.1016/j.ejmech.2012.12.050
35. C.I. Lino, I. Goncalves de Souza, B.M. Borelli, T.T. Silvério Matos, I.N. Santos Teixeira, J.P. Ramos, E. Maria de Souza Fagundes, P. de Oliveira Fernandes, V.G. Maltarollo, S. Johann and R.B. de Oliveira, *Eur. J. Med. Chem.*, **151**, 248 (2018); https://doi.org/10.1016/j.ejmech.2018.03.083
36. H. Osman, S.K. Yusufzai, M.S. Khan, B.M. Abd Razik, O. Sulaiman, S. Mohamad, J.A. Gansau, M.O. Ezzat, T. Parumasivam and M.Z. Hassan, *J. Mol. Struct.*, **1166**, 147 (2018); https://doi.org/10.1016/j.molstruc.2018.04.031
37. N. Ahangar, A. Ayati, E. Alipour, A. Pashapour, A. Foroumadi and S. Emami, *Chem. Biol. Drug Des.*, **78**, 844 (2011); https://doi.org/10.1111/j.1747-0285.2011.01211.x
38. C.B. Mishra, S. Kumari and M. Tiwari, *Eur. J. Med. Chem.*, **92**, 1 (2015); https://doi.org/10.1016/j.ejmech.2014.12.031
39. Leoni A, Locatelli A, Morigi R, Rambaldi M, *Expert Opin. Ther. Patents*, **24**, 201 (2014); https://doi.org/10.1517/13543776.2014.858121
40. P.C. Sharma, K.K. Bansal, A. Sharma, D. Sharma and A. Deep, *Eur. J. Med. Chem.*, **188**, 112016 (2020); https://doi.org/10.1016/j.ejmech.2019.112016
41. A. Puszkiel, G. Noé, A. Bellesoeur, N. Kramkimel, M.-N. Paludetto, A. Thomas-Schoemann, M. Vidal, F. Goldwasser, E. Chatelut and B. Blanchet, *Clin. Pharmacokinet.*, **58**, 451 (2019); https://doi.org/10.1007/s40262-018-0703-0
42. G.M. Keating, *Drugs*, **77**, 85 (2017); https://doi.org/10.1007/s40265-016-0677-x
43. Anuradha, S. Patel, R. Patle, P. Parameswaran, A. Jain and A. Shard, *Eur. J. Pharm. Sci.*, **134**, 20 (2019); https://doi.org/10.1016/j.ejps.2019.04.005
44. Y. Wang, S.W. Chen, G. Hu, J. Wang, W.F. Gou, D.Y. Zuo, Y.C. Gu, P. Gong and X. Zhai, *Eur. J. Med. Chem.*, **143**, 123 (2018); https://doi.org/10.1016/j.ejmech.2017.11.008
45. S.J. Yao, Z.H. Ren, Y.Y. Wang and Z.H. Guan, *J. Org. Chem.*, **81**, 4226 (2016); https://doi.org/10.1021/acs.joc.6b00580
46. E. Lacivita, M. Leopoldo, P.D. Giorgio, F. Berardi and R. Perrone, *Bioorg. Med. Chem.*, **17**, 1339 (2009); https://doi.org/10.1016/j.bmc.2008.12.015
47. R. Maia, R. Tesch and C. Fraga, *Expert Opin. Ther. Pat.*, **22**, 1169 (2012); https://doi.org/10.1517/13543776.2012.719878
48. S.G. O'Brien, F. Guilhot, R.A. Larson, I. Gathmann, M. Baccarani, F. Cervantes, J.J. Cornelissen, T. Fischer, A. Hochhaus, T. Hughes, K. Lechner, J.L. Nielsen, P. Rousselot, J. Reiffers, G. Saglio, J. Shepherd, B. Simonsson, A. Gratwohl, J.M. Goldman, H. Kantarjian, K. Taylor, G. Verhoef, A.E. Bolton, R. Capdeville and B.J. Druker, *N. Engl. J. Med.*, **348**, 994 (2003); https://doi.org/10.1056/NEJMoa022457
49. A. Morikawa and N.L. Henry, *Clin. Cancer Res.*, **21**, 3591 (2015); https://doi.org/10.1158/1078-0432.CCR-15-0390
50. C. Pavlovsky, O. Chan, C. Talati and J. Pinilla-Ibarz, *Future Oncol.*, **15**, 257 (2019); https://doi.org/10.2217/fon-2018-0371
51. P. Anand and B. Singh, *Mini Rev. Med. Chem.*, **14**, 623 (2014); https://doi.org/10.2174/1389557514999140728102737
52. S. Routier, J.L. Bernier, J.P. Catteau, J.F. Riou and C. Bailly, *Anticancer Drug Des.*, **13**, 407 (1998).
53. P. De Isabella, M. Palumbo, C. Sissi, N. Carenini, G. Capranico, E. Menta, A. Oliva, S. Spinelli, A.P. Krapcho, F.C. Giuliani and F. Zunino, *Biochem. Pharmacol.*, **53**, 161 (1997); https://doi.org/10.1016/S0006-2952(96)00646-6
54. A.H. Abdullah, N.S. Ibrahim, F.K. Algethami, A.H. Elwahy, I.A. Abdelhamid and M.E. Salem, *J. Mol. Struct.*, **1302**, 137506 (2024); https://doi.org/10.1016/j.molstruc.2024.137506
55. E.T. Warda, I.A. Shehata, M.B. El-Ashmawy and N.S. El-Gohary, *Bioorg. Med. Chem.*, **28**, 115674 (2020); https://doi.org/10.1016/j.bmc.2020.115674
56. T. Khan, K. Sankhe, V. Suvarna, A. Sherje, K. Patel and B. Dravyakar, *Biomed. Pharmacother.*, **103**, 923 (2018); https://doi.org/10.1016/j.biopha.2018.04.021
57. M.S. Sinicropi, J. Ceramella, P. Vanelle, D. Iacopetta, O. Khoumeri, C. Rosano, S. Abdelmohsen, W. Abdelhady and H. El-Kashef, *Pharmaceuticals*, **16**, 946 (2023); https://doi.org/10.3390/ph16070946
58. A.K. McClendon and N. Osheroff, *Mutat. Res.*, **623**, 83 (2007); https://doi.org/10.1016/j.mrfmmm.2007.06.009
59. R. Gali, J. Banothu, M. Porika, R. Velpula, R. Bavantula and S. Abbagani, *RSC Adv.*, **4**, 53812 (2014); https://doi.org/10.1039/C4RA11428K
60. V. Unadkat, S. Rohit, P. Parikh, K. Patel, V. Sanna and S. Singh, *OncoTargets Ther.*, **2**, 479 (2022); https://doi.org/10.2147/OTT.S357765
61. http://autodock.scripps.edu/resources/references
62. Discovery Studio Modeling Environment, Release 4.1.0, Accelrys Software Inc.: San Diego, California, USA (2013).
63. A.D. Becke, *J. Chem. Phys.*, **98**, 5648 (1993); https://doi.org/10.1063/1.464913
64. C. Lee, W. Yang and R.G. Parr, *Phys. Rev. B Condens. Matter*, **37**, 785 (1988); https://doi.org/10.1103/PhysRevB.37.785
65. N. Kavitha, M. Alivelu and T. Savithajyostna, *Chem. Phys. Impact*, **8**, 100602 (2024); https://doi.org/10.1016/j.chphi.2024.100602
66. C.C. Wu, T.K. Li, L. Farh, L.Y. Lin, T.S. Lin, Y.J. Yu, Y. Tj, C.W. Chiang and N.L. Chan, *Science*, **333**, 459 (2011); https://doi.org/10.1126/science.1204117
67. C.C. Wu, T.K. Li, L. Farh, L.-Y. Lin, T.-S. Lin, Y.-J. Yu, T.-J. Yen, C.-W. Chiang and N.-L. Chan, *Science*, **333**, 459 (2011); https://doi.org/10.1126/science.1204117
68. R. Palabindela, R. Guda, G. Ramesh, P. Myadaraveni, D. Banothu, G. Ravi, R. Korra, H. Mekala and M. Kasula, *J. Heterocycl. Chem.*, **59**, 1533 (2022); https://doi.org/10.1002/jhet.4488
69. Y.B. Shankar Rao, M.V.S. Prasad, N. Udaya Sri and V. Veeraiah, *J. Mol. Struct.*, **1108**, 567 (2016); https://doi.org/10.1016/j.molstruc.2015.12.008
70. B.S. Iyengar, R.T. Dorr, D.S. Alberts, A.M. Sólyom, M. Krutzsch and W.A. Remers, *J. Med. Chem.*, **40**, 3734 (1997); https://doi.org/10.1021/jm970308+
71. X. Zhang, Z. Chi, J. Zhang, H. Li, B. Xu, X. Li, S. Liu, Y. Zhang and J. Xu, *J. Phys. Chem. B*, **115**, 7606 (2011); https://doi.org/10.1021/jp202112e
72. M. Manju, S. Suresh, P.A. Vivekanand, S. Gunasekaran, S. Srinivasan and C.S. Biju, *Mater. Today Proc.*, **36**, 857 (2021); https://doi.org/10.1016/j.matpr.2020.07.018
73. M. Pramanik, N. Chatterjee, S. Das, K.D. Saha and A. Bhaumik, *Chem. Commun.*, **49**, 9461 (2013); https://doi.org/10.1039/c3cc44989k
74. M. Govindarajan, M. Karabacak, V. Udayakumar and S. Periandy, *Spectrochim. Acta A Mol. Biomol. Spectrosc.*, **88**, 37 (2012); https://doi.org/10.1016/j.saa.2011.11.052
75. A. Daina, O. Michielin and V. Zoete, *Sci. Rep.*, **7**, 42717 (2017); https://doi.org/10.1038/srep42717
76. M.J. Waring, J. Arrowsmith, A.R. Leach, P.D. Leeson, S. Mandrell, R.M. Owen, G. Pairaudeau, W.D. Pennie, S.D. Pickett, J. Wang, O. Wallace and A. Weir, *Nat. Rev. Drug Discov.*, **14**, 475 (2015); https://doi.org/10.1038/nrd4609